Fall 1997

Characteristics of recycled plastics and applications for highway appurtenances

Keith MacBain
New Jersey Institute of Technology

ABSTRACT

CHARACTERISTICS OF RECYCLED PLASTICS AND APPLICATIONS FOR HIGHWAY APPURTENANCES

by
Keith MacBain

Recycling is gaining widespread support in many communities as an environmentally acceptable solution to the management of solid waste. The success of these recycling programs depends largely on the development of high-value end use for the recycled products. This research involves an experimental and analytical study on the development of high-value, high-volume end uses for recycled plastic shapes. The experimental part includes material tests to determine mechanical properties of various recycled plastics. A constitutive model is proposed and verified that can be used in characterization of recycled plastics. Bending tests of recycled plastic beams were performed to assess strength, stiffness and mode of failure. Analytical results using the proposed constitutive model are in good agreement with the experimental results. An innovative noise wall design that takes advantage of multi-layering to increase stiffness and sound effectiveness is discussed as well as other possible uses and future research needs.

CHARACTERISTICS OF RECYCLED PLASTICS AND APPLICATIONS FOR HIGHWAY APPURTENANCES

by
Keith MacBain

A Thesis
Submitted to the Faculty of
New Jersey Institute of Technology
in Partial Fulfillment of the Requirements for the Degree of
Master of Science in Civil Engineering

Department of Civil and Environmental Engineering

October 1997

APPROVAL PAGE

CHARACTERISTICS OF RECYCLED PLASTICS AND APPLICATIONS FOR HIGHWAY APPURTENANCES

Keith MacBain

Dr. M. Ala Saadeghvaziri, Thesis Advisor   Date
Associate Professor of Civil Engineering, NJIT

Prof. Edward G. Dauenheimer, Committee Member   Date
Professor of Civil and Environmental Engineering, NJIT

Dr. William Spillers, Committee Member   Date
Distinguished Professor of Civil and Environmental Engineering, NJIT

BIOGRAPHICAL SKETCH

Author: Keith MacBain

Degree: Master of Science

Date: October 1997

Undergraduate and Graduate Education:

- Master of Science in Structural Engineering,
  New Jersey Institute of Technology, Newark, NJ, 1997

- Bachelor of Science in Civil Engineering.
  New Jersey Institute of Technology, Newark, NJ, 1996

Major: Civil Engineering

To my beloved family

ACKNOWLEDGMENT

TABLE OF CONTENTS

TABLE OF CONTENTS
(Continued)

LIST OF TABLES

LIST OF FIGURES

LIST OF FIGURES
(Continued)

CHAPTER 1

INTRODUCTION

1.1 Background

Solid waste is overloading the landfills and is a major contributor to the environmental problems facing this country. Every year the U.S. alone generates 320 billion lb (145 billion kg.) of municipal solid waste. Of this waste, plastics comprise 18 percent by volume and 7 percent by weight [1]. Furthermore, plastics and paper are the fastest growing segments of solid wastes [2].

Recycling is an environmentally acceptable means of reducing solid waste and conserving resources. Reprocessing industrial plastic waste (e.g., in-house scrap) has been a common practice for as long as the plastic industry has existed. There have recently been significant developments in the recycling technology of commingled plastic waste but the key issue to be resolved is securing long-term, high-value markets for recycled polymers.

This research investigates some of the products of the recycled plastic industry to evaluate their mechanical and structural properties and to assess conformity of these properties among manufacturers. The use of recycled plastics in development of economical and environmentally acceptable highway appurtenances, such as noise and traffic barriers, is also discussed.

1.2 General Properties of Recycled Plastics

Mixed, or commingled, plastics once destined for the waste stream are now being recycled [3]. Collected plastic scrap is granulated, then melted and processed in an extruder. The molten plastic is then forced into a mold cavity of the shape and size of the final product. The product can be cut and shaped with the same tools and fastening devices used for wood. These molded products are resistant to attack from gas, oil, salt, sunlight, chemicals and insects and will withstand human and mechanical abuse [4]. Test results have shown mixed plastics hold nails approximately 40 percent better than wood [5]. Fiberglass and treated wood fiber, both classified as hazardous waste materials, have been successfully used to improve the mechanical properties [6] of recycled plastics.

Currently, molded shapes are used to make park benches, guardrail block outs, fences, road markers, landscape timbers and a wide variety of other non-structural applications. Although it has been highly anticipated that molded shapes "will replace wood, concrete and steel" [7], structural applications of the product are practically non-existent. This is mainly due to lack of knowledge about the mechanical and structural properties of the material, especially their relation to long term performance. Lack of testing standards and design specifications compound the problem.

Previous work [8] has revealed that the modulus of elasticity varies greatly among manufacturers. Creep effects [9] are thought to be significant and it has been noted [10] that sample size and temperature affect material properties. It has also been shown [11] that these recycled plastics are virtually non-toxic which is in sharp contrast to chemically pressure treated lumber

CHAPTER 2

EXPERIMENTAL TESTS

The cross-section of the standard recycled plastic (RP) lumber shape is visually non-homogeneous, suggesting that the material properties also vary. Non-homogeneity of the material is attributed to the cooling process during extrusion; the section normally cools from the outside first causing the periphery to solidify before the center. Shrinkage of the center as it cools can also distort the final form of the section causing rounded corners and uneven surfaces. Although the degree of variation is different for various manufacturers and shapes, all products evaluated depict this phenomenon. Material tests (tension and compression) were conducted to investigate this difference and the results were used to formulate a constitutive model for RP that can be employed in analytical studies. To validate the constitutive model and to assess global behavior of structural components (such as stiffness, strength, and ductility) member tests in bending were performed and the results were compared with the analytical results using the proposed material model.

There is currently no industry standard for the manufacture of RP products so there is variation among the manufacturers in composition as well as the methods of acquiring materials. To represent the range of compositions available, three manufacturers (to be called A, B & C) were selected for testing. Manufacturer A mixes fiberglass with the RP, B uses only RP, and C uses 50% wood fiber in addition to the RP. It must be mentioned that variations in material strength among manufacturers are not a problem in developing structural applications, but consistency (reliability) of the mechanical properties and long term performance are.

The cross section of the extruded product can have any shape but only standard lumber shapes (2x10, 4x4, and 6x6) were used in testing because these are commonly produced. The actual dimensions of the 2x10, 4x4, and 6x6 are approximately 1.5" x 9.5", 3.5" x 3.5", and 5.5" x 5.5" respectively but they are generally referred to by their nominal size.

2.1 Material Tests

Material tests were performed to asses the variation of material properties within the material as well as the variation among manufacturers.

2.1.1 Selection of Coupons

To investigate the apparent non-homogeneity, visually consistent sections were cut from both 4x4 and 6x6 shapes and termed 'core' or 'shell' coupons based on their origin. Coupons were also cut from 2x10 shapes but the visually consistent shell section was too thin (typically less than 0.4") to be used for standard coupons. The core and shell coupons were not only visually different but also were noted to have different dry densities after they were weighed and measured. The dry density of the shell coupons was found to range between 57 to 68 pounds per cubic foot. Depending on manufacturer (and lumber size for Manufacturer B), the core coupons typically had 50% the density of the shell.

2.1.2 Specimen Dimensions and Test Set Up

Core and shell coupons for tension tests were 0.5" x 1.57" x 8" nominal and the compression coupons were 0.5" x 1.57" x 0.79" nominal. Since ASTM is still developing

RP test standards, procedures for wood and plastic were used. Ten tension tests were conducted similar to ASTM D 638 and ten compression tests were conducted observing ASTM D 695 for each manufacturer. Tension strain was measured with a clip-on type gage over a 2" initial gage length and the load was recorded.

2.1.3 Results

Figures 2.1 through 2.3 show tension and compression stress-strain diagrams for both core and shell coupons for all three manufacturers. Stress was computed by dividing the recorded load by the original cross sectional area. The compression test results are plotted only to a maximum of 10% strain because all materials began to visually fail near this point. It should be noted that beyond 30% strain, the materials exhibit hyper-elastic behavior; there was no point of maximum stress but rather the stress continued to increase after the material visually failed. This was also characterized by a softening (lower modulus of elasticity) followed by a stiffening of the material. Figure 2.4 shows a typical full scale compression test for Manufacturer B which marks the point of inflection (change in curvature) and indicates the minimum stiffness. This stiffening is likely attributed to the size of the sample used rather than it being representative of true material characteristics for large deformations. For rectangular wood samples, ASTM recommends that the height be no greater than two times the minimum thickness but it is believed that these recommendations are not appropriate for compression testing of plastics where large deformations are expected. The coupons appeared to be approaching a point that would require the material to undergo viscous flow for continued deformation which is, of course, entirely apart from the objective of these tests. The results of this method are
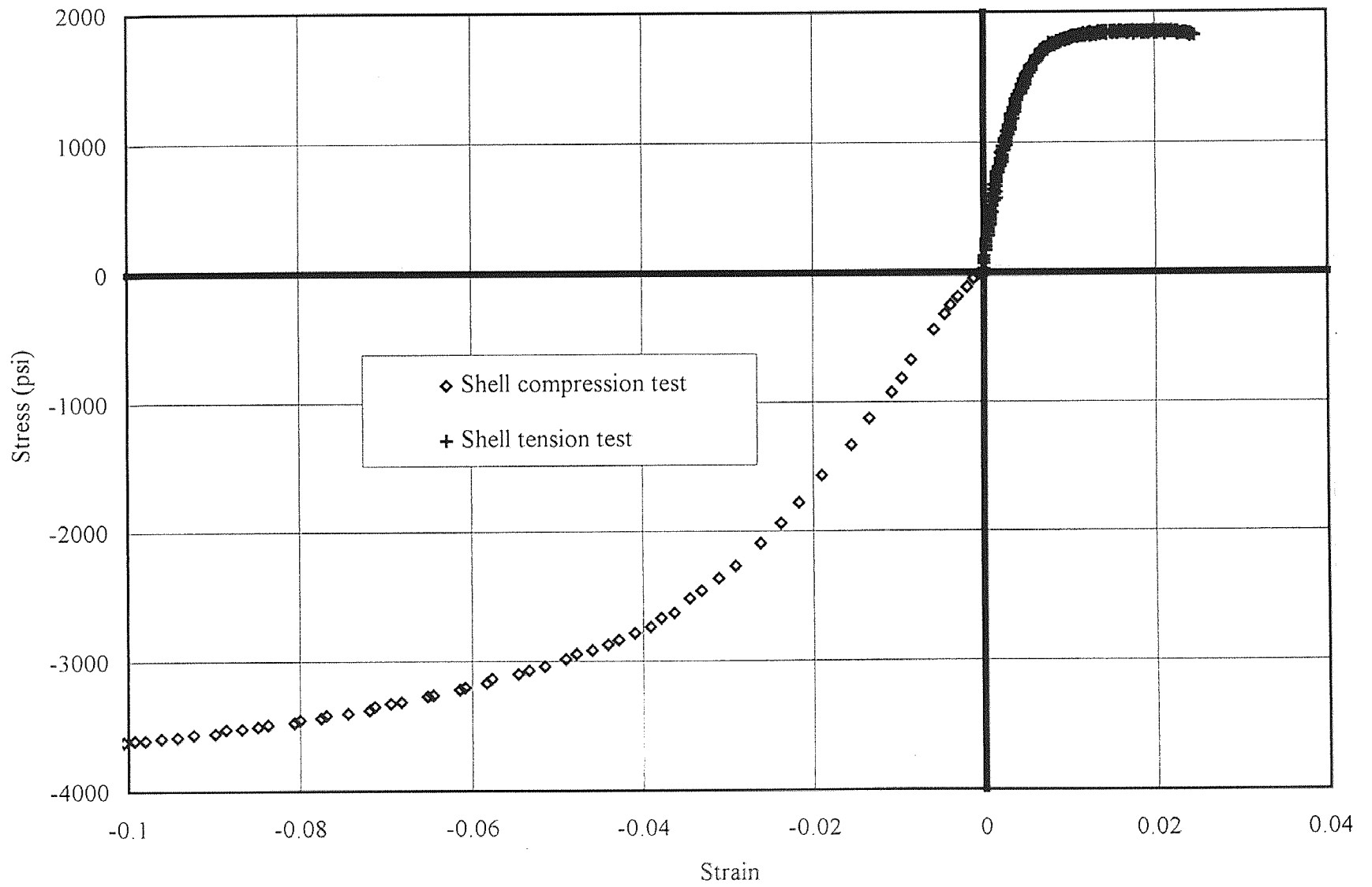
Figure 2.1 Material Properties for Manufacturer A
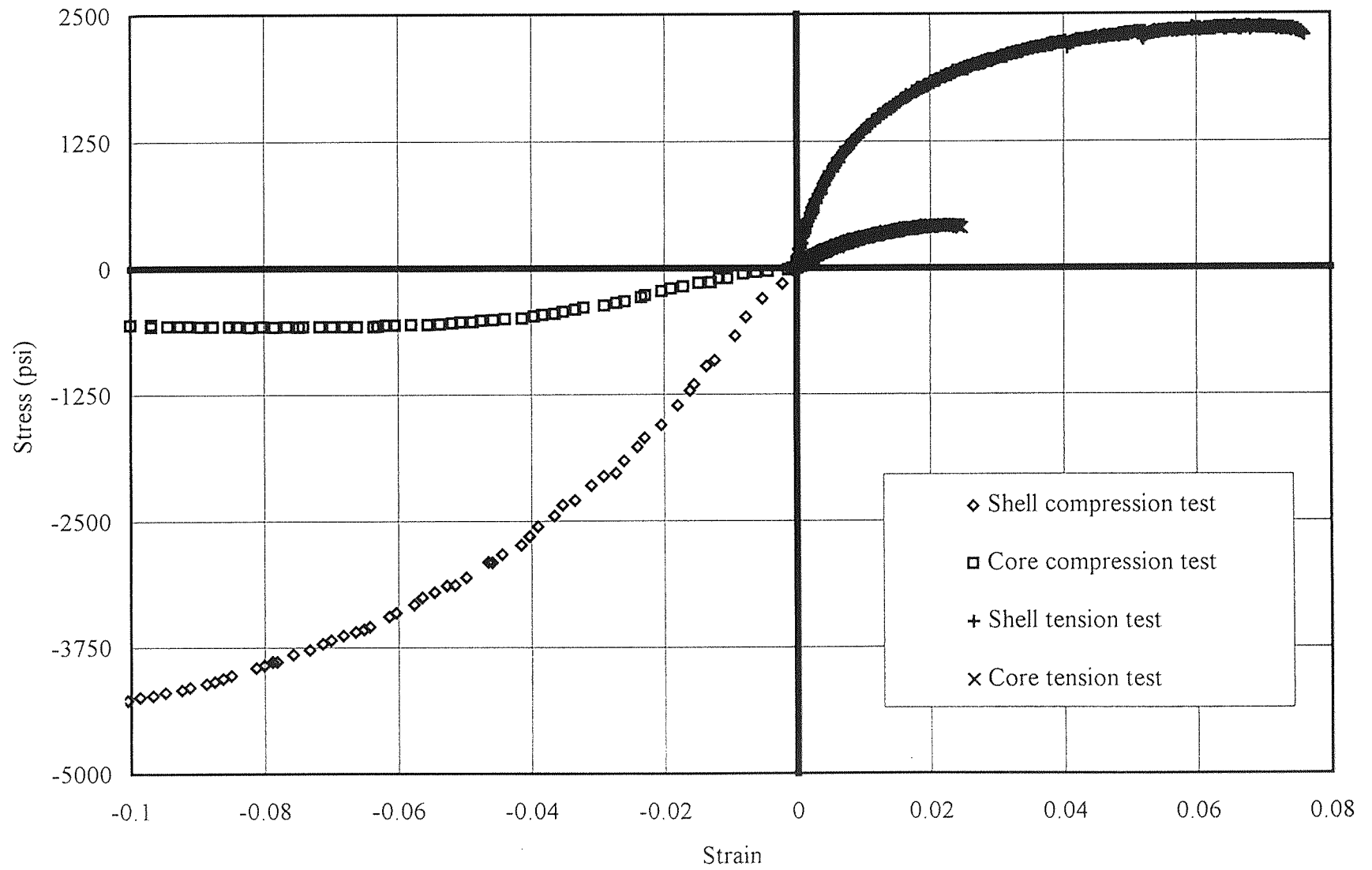
Figure 2.2 Material Properties for Manufacturer B
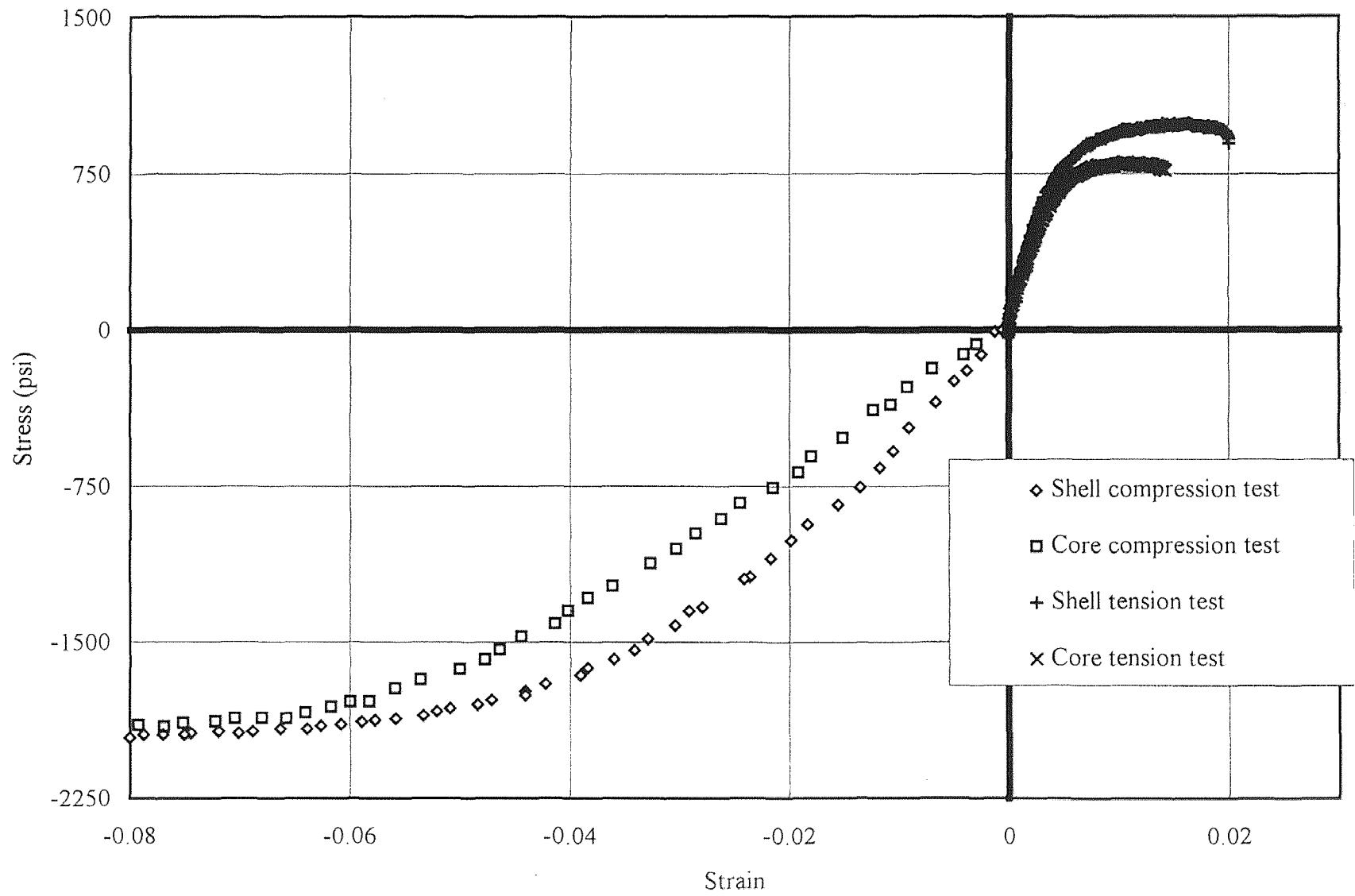
Figure 2.3 Material Properties for Manufacturer C
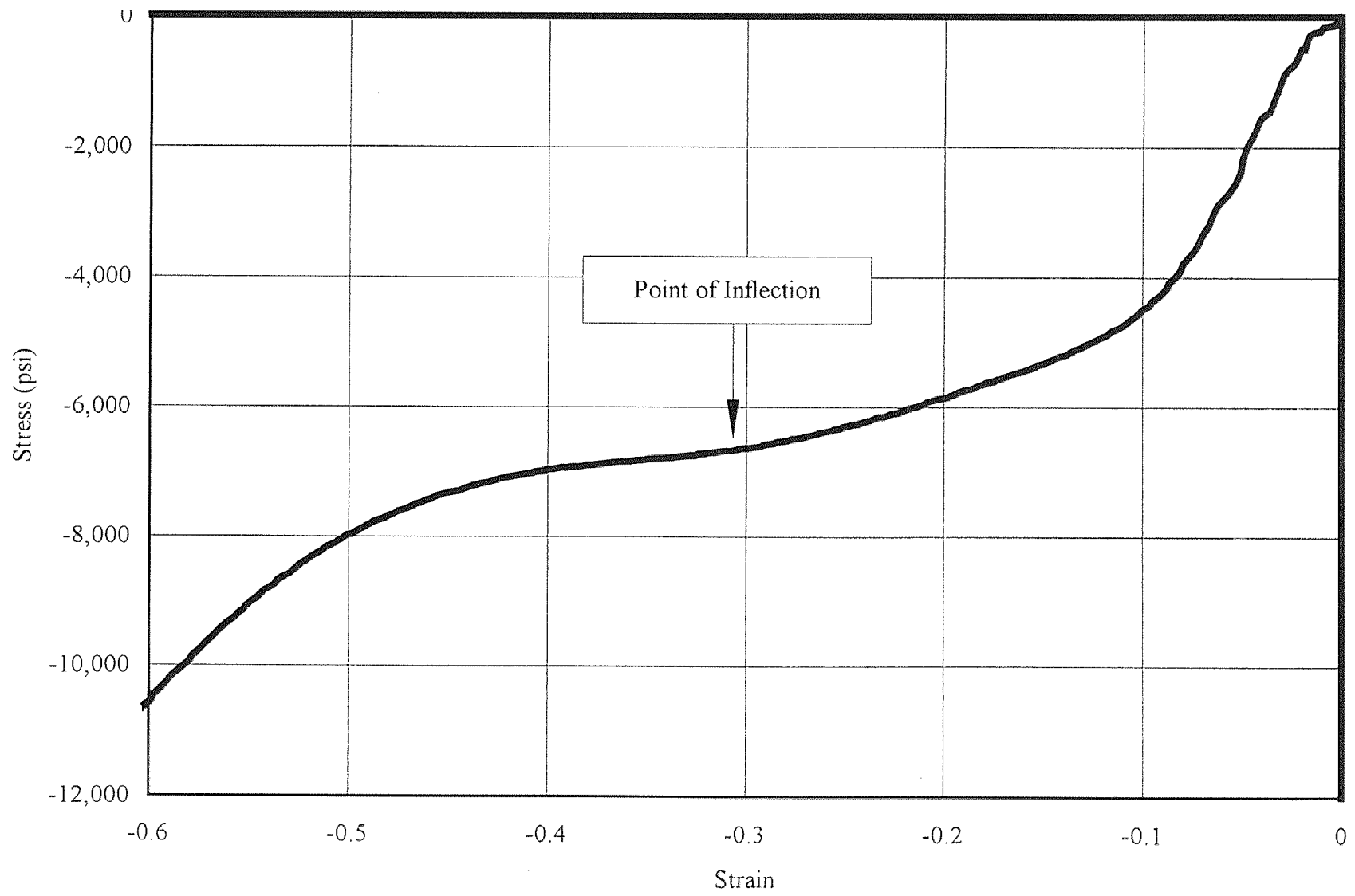
Figure 2.4 Full Scale Compression Test, Manufacturer B

applicable for small to moderate strain (less than 10%) but if large deformation results are desired, a different sample size may provide more representative results.

The stress-strain diagrams show that there is a significant difference in both the tension and compression behavior as well as the core and shell materials. It can also be seen that the material is non-linear throughout its range. For all manufacturers tested, the core was found to have lower initial tangent modulus of elasticity (E) and lower ultimate strength. Manufacturer A foam-fills the core for aesthetic purposes so these materials were not tested. Table 2.1 shows the variation in material properties between shell and core coupons in tension and compression for all three manufacturers tested. For Manufacturer B, the material properties varied with the size of the section. The core coupons from 4x4 sizes had a smaller E than that of the 6x6 and 6x8. It was also noted that the core density of the 4x4 (23 pcf) was nearly half that of the 6x6 and 6x8 (42 pcf). This suggests a correlation between density and stiffness; higher density corresponds to a higher stiffness but variations in density of less than 5% do not appear significant. Although it is unclear if Manufacturer B uses different raw materials to form different shapes, it is thought that the variation in density and stiffness is caused by the size and shape of the section. While it is beyond the scope of this paper, the rate of cooling is thought to have an important effect on the material properties and because the section will cool from the outside first, the shell will impose boundary conditions on the core as it cools. Noting that only the core properties vary for different sizes and that the 6x6 and 6x8 have the same minimum center to perimeter distance supports this notion.

Table 2.1 Material Properties

Manufacturer and type		E_t (ksi)	E_c (ksi)	max tension stress (psi)	compression stress at inflection point (psi)
A	Shell	625	125	1800	3250
	Core	NA	NA	NA	NA
B	Shell	270	100	2200	5100
	(4x4) Core	51	35	580	1000
	(6x6, 6x8) Core	150	72	750	1300
C	Shell	320	90	1000	2000
	Core	260	65	750	1900

Coupons from all manufacturers were seen to contain varying amounts of impurities; tension failure usually occurred at these locations. Impurities are typically materials such as bottle tops that are inadvertently collected and granulated with the recyclables but melt at a different (normally higher) temperature. The amount of bond adhesion for these impurities is unknown. The size of the impurities varied, but typically comprised less than 5% of the cross-sectional area for A and C while they contributed as much as 10% for B. This is believed to be a factor in the divergence from theory mentioned in later sections.

2.1.4 Proposed Constitutive Model

Based on analyses of the test results under both tension and compression stresses for all manufacturers, the following equation is proposed to define material characteristics of recycled plastics:

$$\sigma = \frac{A\,\varepsilon}{B\,\varepsilon^2 + C\,\varepsilon + D}$$

where σ represents the stress, ε represents the strain, and A, B, C, and D are material constants.

The material constants need to be determined for each type of material; that is, tension and compression of core and shell. This requires sixteen constants for each manufacturer to fully define the section behavior. These constants were determined using a method that attempts to minimize Chi-square [12] as implemented by Temple Graph software. The model was not fit to the compression curves beyond the point of inflection.

For all three manufacturers the proposed model can simulate the experimental results with high accuracy. In Figure 2.5, a stress-strain diagram from material tests of Manufacturer B is plotted along with the proposed model, which shows a good match. Table 2.2 lists the material constants for all three manufacturers (ε is dimension-less and σ is in psi). These results were used to simulate member response and compared to experimental results as discussed in the following sections.
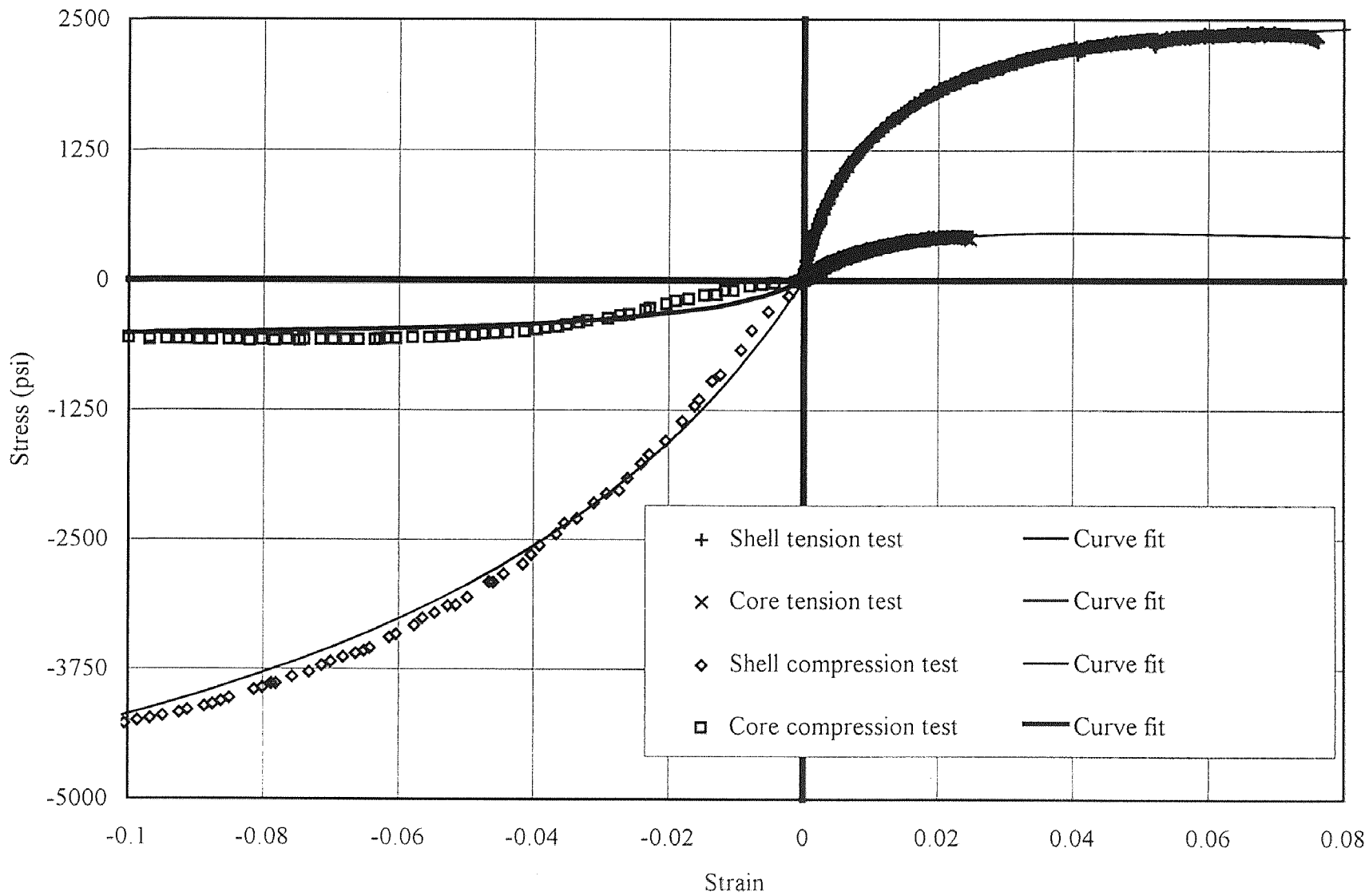
Figure 2.5 Material Properties and Curve-fit for Manufacturer B

Table 2.2 Material Constants

Manufacturer & coupon		A	B	C	D
A	Shell - tension	2.55E+7	1.68E+3	8.49E+3	40
	Shell - compression	2.45E+8	7.24E+4	-4.33E+4	1.94E+3
	Core - tension	0	0	0	1
	Core - compression	0	0	0	1
B	Shell - tension	1.69E+7	2.46E+3	6.04E+3	62
	Shell - compression	3.70E+8	-5.39E+3	-5.19E+4	3.70E+3
	Core - tension	1.37E+7	1.47E+5	1.77E+4	264
	Core - compression	1.25E+8	7.81E+4	-1.99E+5	3.87E+3
C	Shell - tension	2.02E+7	2.98E+5	1.21E+4	62
	Shell - compression	1.21E+8	1.16E+5	-3.99E+4	1.36E+3
	Core - tension	2.01E+7	7.28E+5	1.03E+4	77
	Core - compression	1.39E+8	8.70E+4	-4.68E+4	2.11E+3

2.1.5 Freeze / Thaw Exposure

To help asses the effects of long term outdoor exposure, all materials were exposed to

freeze / thaw cycles. Standard tension and compression coupons were submerged in

water for six days and then put into a chamber that regulated the temperature. One cycle

consisted of at least 12 hours frozen (-60° F) and at least 12 hours thawed (68° F). The

relative humidity was between 65% and 75% at all times. All coupons were subjected to

at least 60 freeze / thaw cycles before performing the same material tests as before.

Referring to Figures 2.6 through 2.8, it can be seen that strength and stiffness were

reduced in materials containing wood fibers (Manufacturer C) while those containing all

plastic (Manufacturer B) or mixed with fiberglass (Manufacturer A) were not affected

significantly. This indicates that plastics containing wood fibers are not a good choice for

long term outdoor exposure where structural considerations are important.
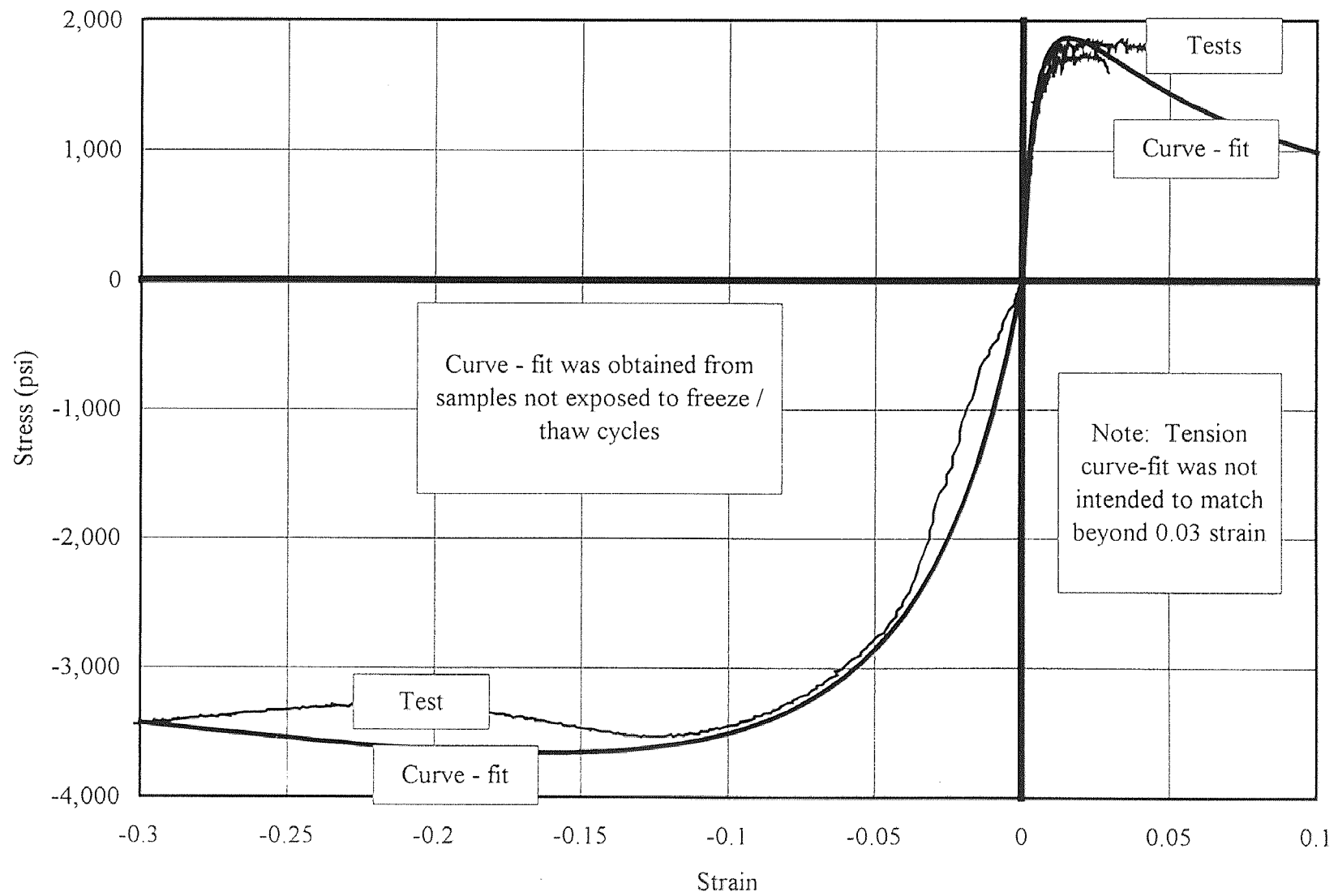
Figure 2.6 Freeze / Thaw Tests Compared with Curve-fit Results, Manufacturer A
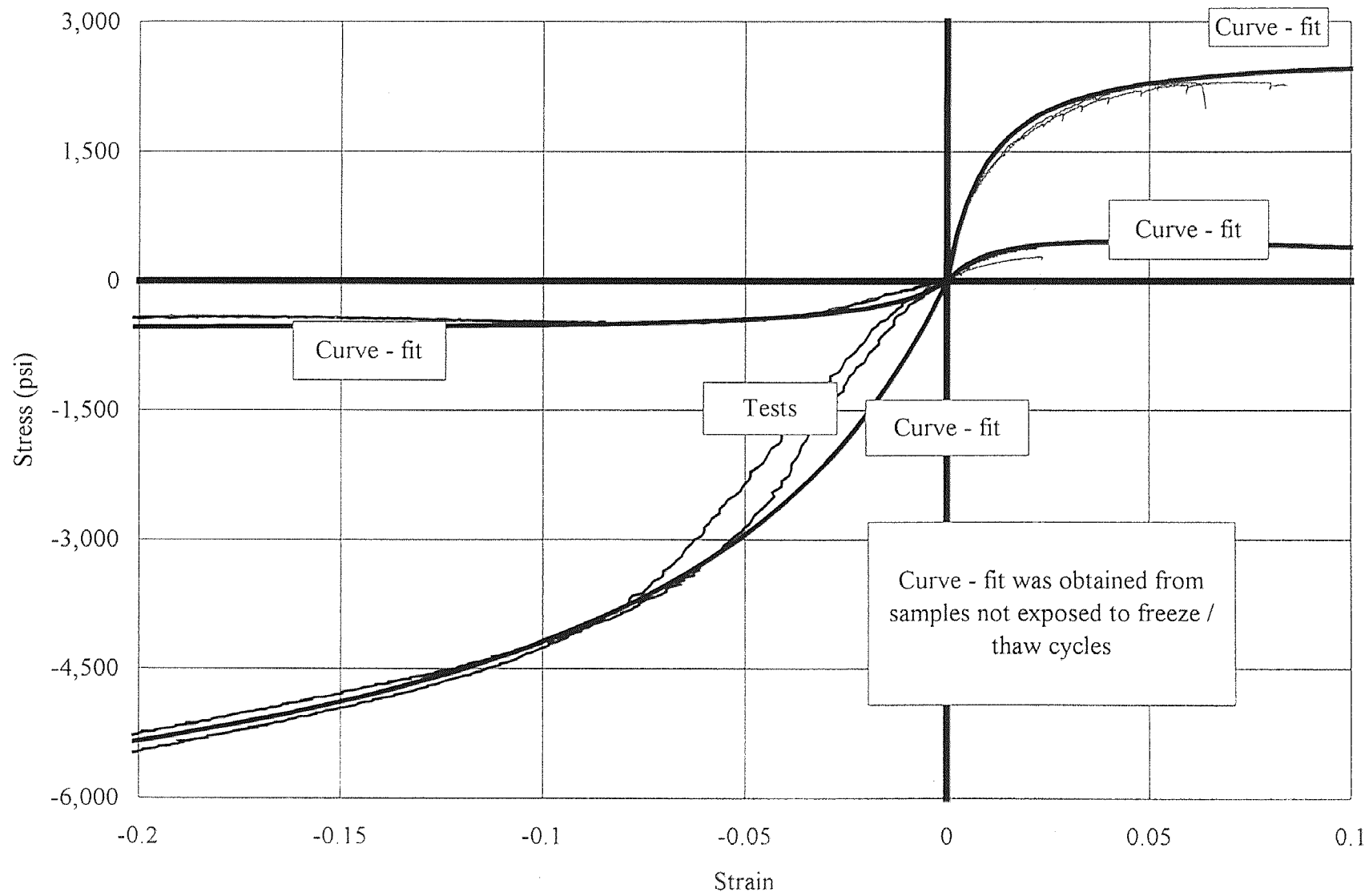
Figure 2.7 Freeze / Thaw Tests Compared with Curve-fit Results, Manufacturer B
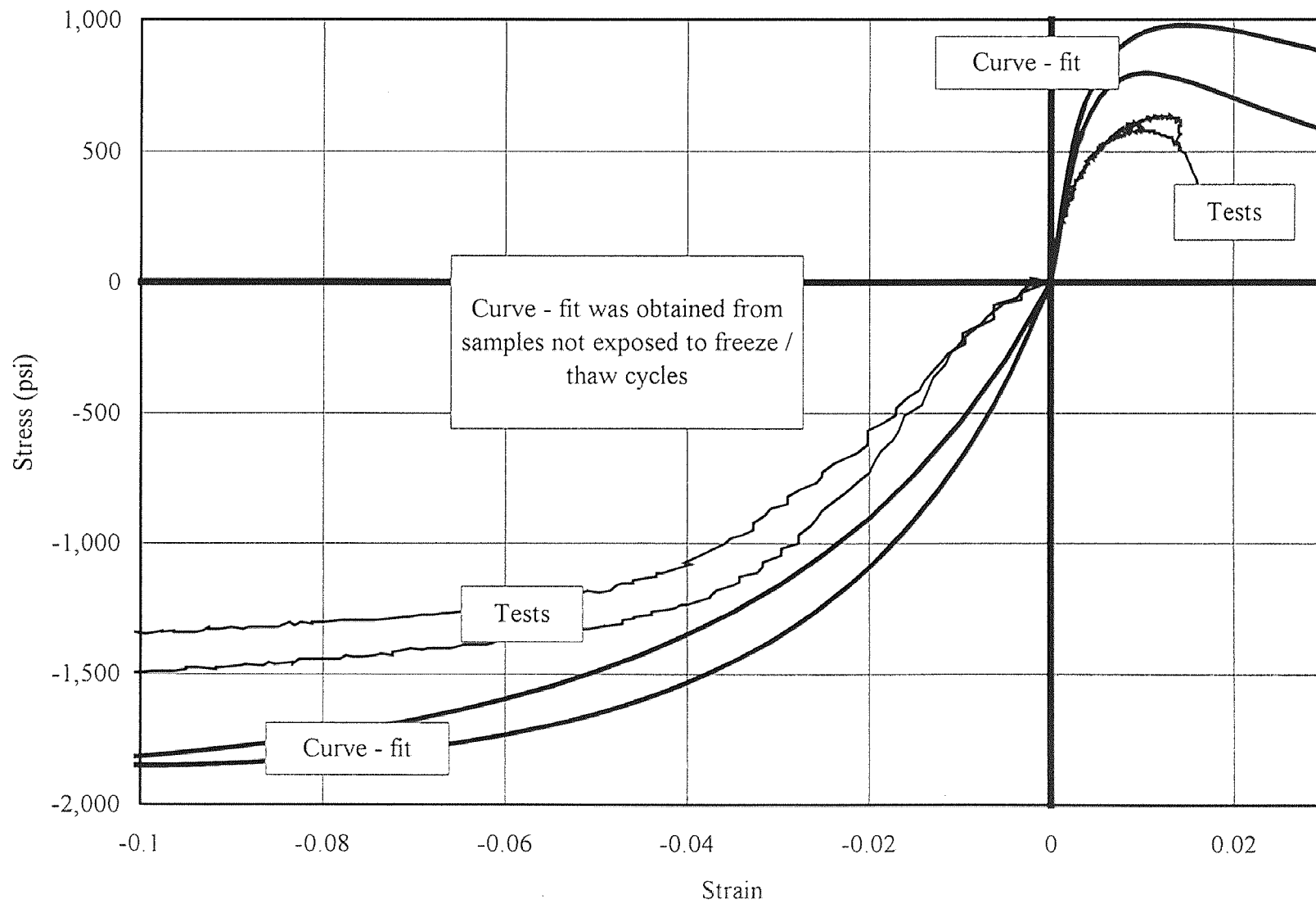
Figure 2.8 Freeze / Thaw Tests Compared with Curve-fit Results, Manufacturer C

2.1.6 Creep

Standard compression coupons were subjected to a constant dead load that produces a stress level of 10 psi. This is a typical dead load stress level at the base of a 20 ft high wall created with RP. The temperature was held constant at 95° F throughout. Figure 2.9 shows that after 7 months, the creep strain for all manufacturers was less than 0.15% and that no creep strain has been measured in the last 4 months for Manufacturer A. If this strain were (conservatively) considered constant throughout the height, it equates to a creep deflection of only 0.3 inch for a 20 ft high wall. Although this is acceptable for a noise wall, Table 2.3 shows it is extremely large when compared to the initial strain obtained from the test data. Creep deflection comprises the larger portion of the total deflection by far, even for low stress levels. Noting that 10 psi is at least 15 times less than the ultimate compressive stress found in the material tests for all manufacturers, it is apparent that creep deflection can be very significant and is discussed further in Section 5, Future Work.

Table 2.3 Summary of Creep Strain

Manufacturer	Initial strain (%)	Creep strain after 7 months (%)	Increase from initial strain
A	0.008	0.13	1625 %
B	0.01	0.13	1300 %
C	0.01	0.13	1300 %
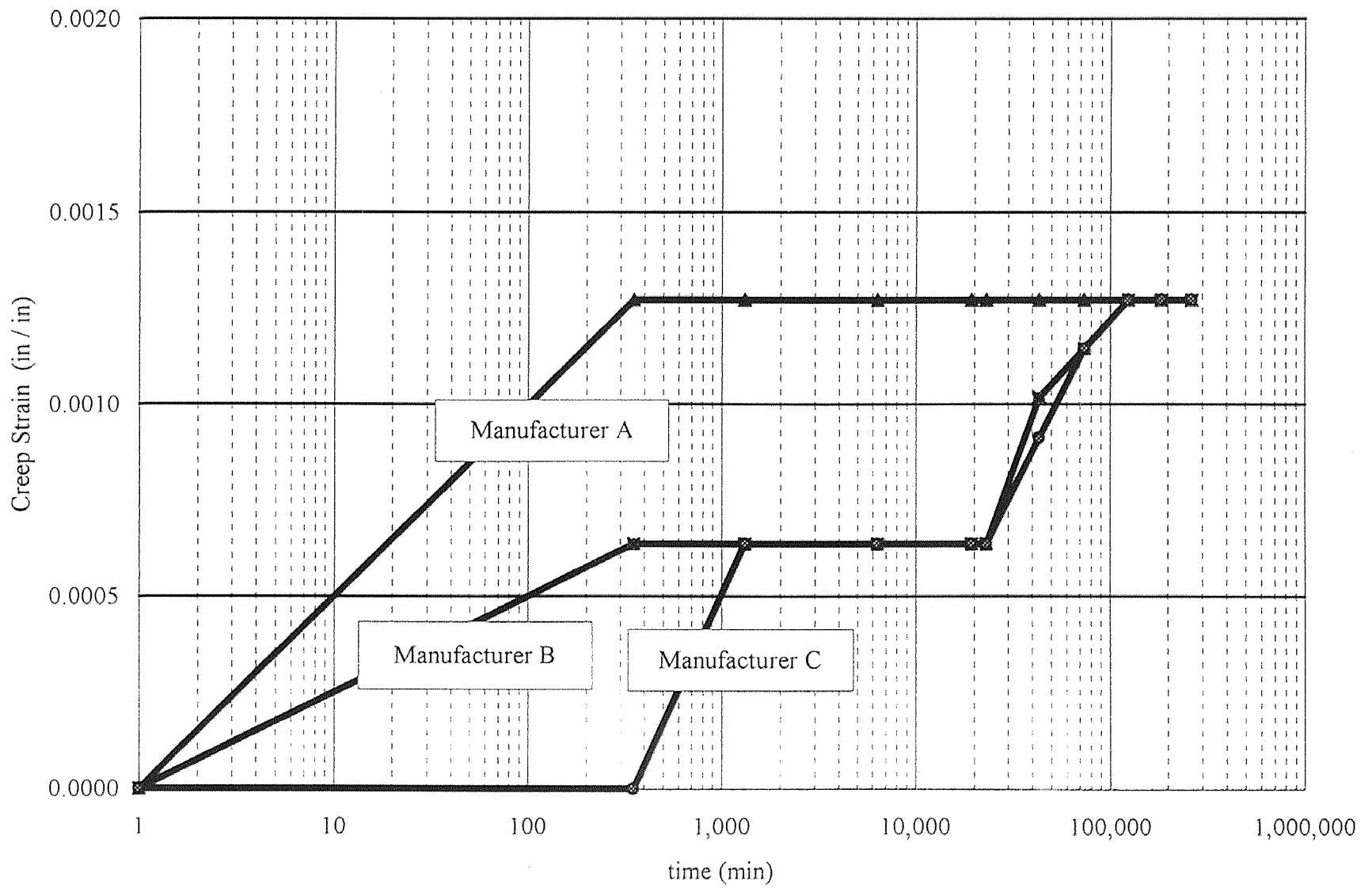
Figure 2.9 Creep Strain vs Time

2.2 Member Tests

2.2.1 Test Setup and Specimens

Four-point bending tests were performed on 27" long 4x4 samples in accordance with ASTM D 198. In addition to load and deformation at the load point, outer fiber strain was recorded using strain gages adhered to the top and bottom of the member before testing. End rotation was also recorded using dial gages. Three point bending tests were conducted on 60" long 6x6 and 6x8 sections although outer fiber strain and end rotation were not recorded for the larger sections. Three 4x4's, one 6x6 and one 6x8 were tested from each manufacturer.

Axial compression tests were performed on whole 4x4 sections with an initial height of 4.5". Four samples were used for each manufacturer and testing proceeded following ASTM D 198, Static Compression of Timbers in Structural Sizes.

2.2.2 Flexural Test Results

The load deformation results show non-linear behavior similar to the material tests. An interesting observation is that despite significant differences in material properties for tension and compression (Figures 2.1 through 2.3), the strain at the top and bottom outer fibers were within 25% of each other for all specimens tested. Figure 2.10 shows the strain at the top and bottom outer fibers as the bending moment increases at mid-span of a 4x4 for Manufacturer B. Because the data acquisition equipment was not able to record two independent signals simultaneously, the signals from the top and bottom strain gages were recorded alternately for short intervals causing the gaps in the plot. When the RP section is in flexure, the large difference revealed in the material tests between tension and

25,000

20,000

Moment (in-lb)

15,000

10,000

5,000

0

Test

Theory

Compression
Strain at Top of
Beam

Tension Strain
at Bottom of
Beam

Test

Theory

-0.08   -0.06   -0.04   -0.02   0   0.02   0.04   0.06   0.08   0.1

Strain at Outer Fiber
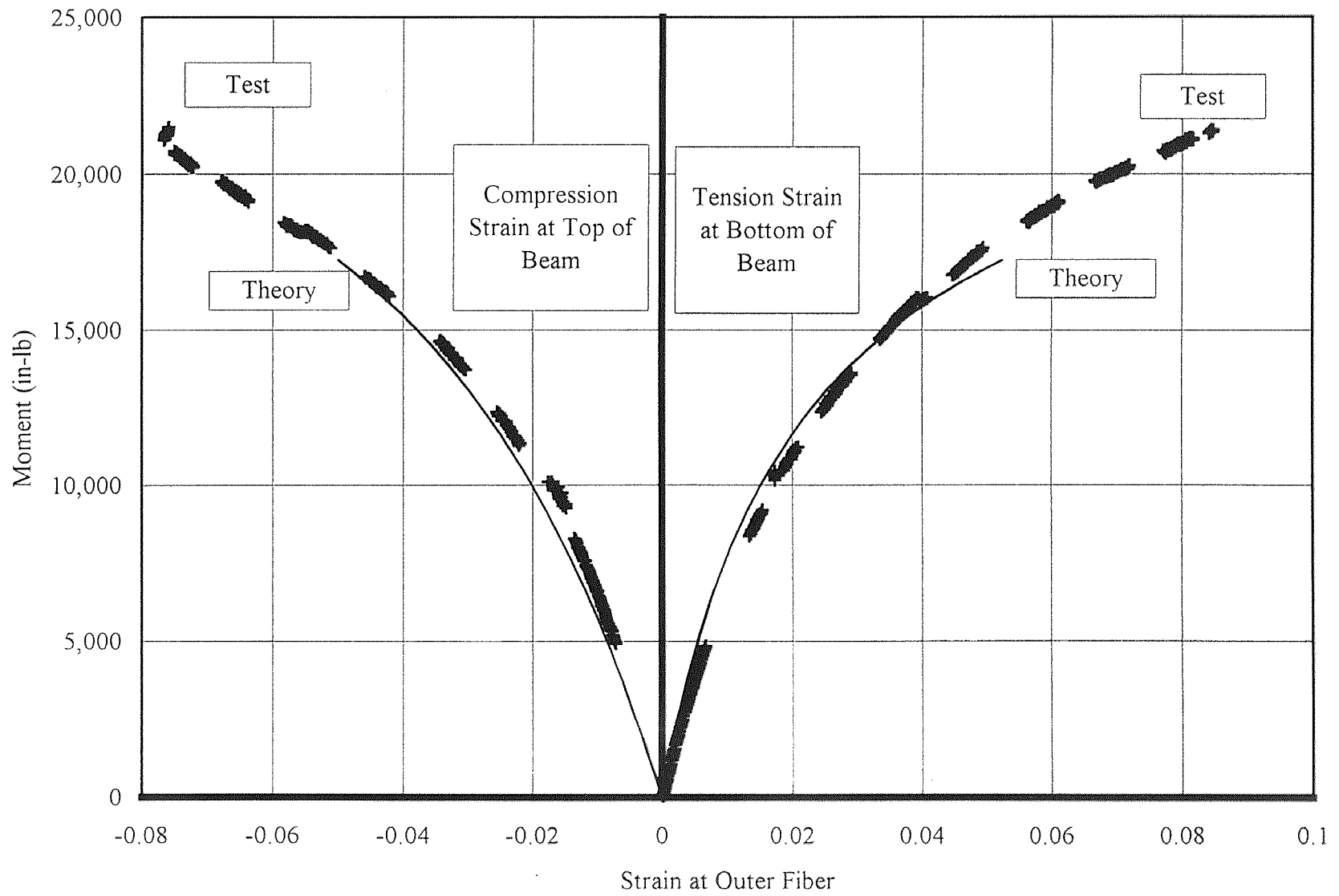
Figure 2.10 Strain at Outer Fiber, Manufacturer B

compression behavior is compensated for by the shifting of the location of zero strain or neutral axis (NA) that occurs during bending. Figure 2.11 illustrates this shift as the moment increases based on the theoretical analysis. Considering a symmetric section, initially the NA is below the geometric centerline because the modulus of elasticity in tension (E_t) is greater than that in compression (E_c). At larger strains, E_t becomes less than E_c and the NA rises to maintain the force equilibrium. That is, tension strain approaches (and may surpass) compression strain because E_c maintains nearly its initial value at strains that E_t has lost most of its initial value and a greater increase in tension strain is needed to balance the force generated by a nominal increase in compression strain. This is consistent with the strains recorded in the 4x4 tests and shown in Figure 2.10.

Although all three products had good ductility for structural purposes, they all failed suddenly as reflected by the lack of a descending portion in the load-deformation curves. Products from Manufacturer B exhibited the largest tension strain (9%) before failure. The greater ductility can be attributed to the lack of reinforcement in the product. That is, addition of fibers (glass or wood) reduces ductility, apparently due to bond failure.

2.2.3 Compression Test Results

The axial compression results showed that all manufacturers exhibited similar behavior. Near the ultimate load for the section, the stiffness dropped considerably and the shell began to buckle away from the core marking visual failure (Figures 2.12(a) and 2.12(b)). The ultimate compressive strength of the member, thus, is affected by not only the height of the section, but also the bond strength between core and shell materials. After visual
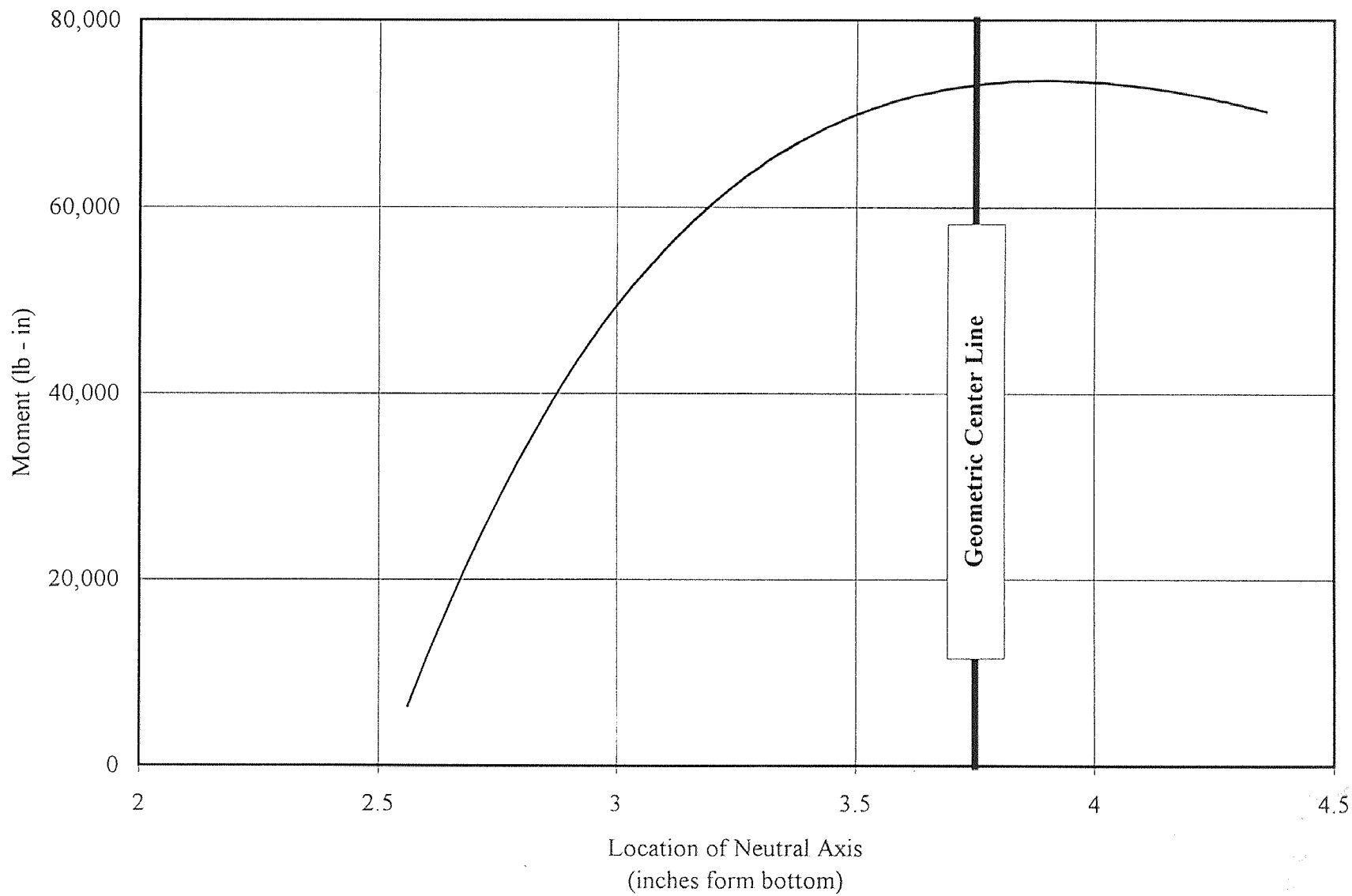
Figure 2.11 Moment vs Neutral Axis, Manufacturer C 6x8
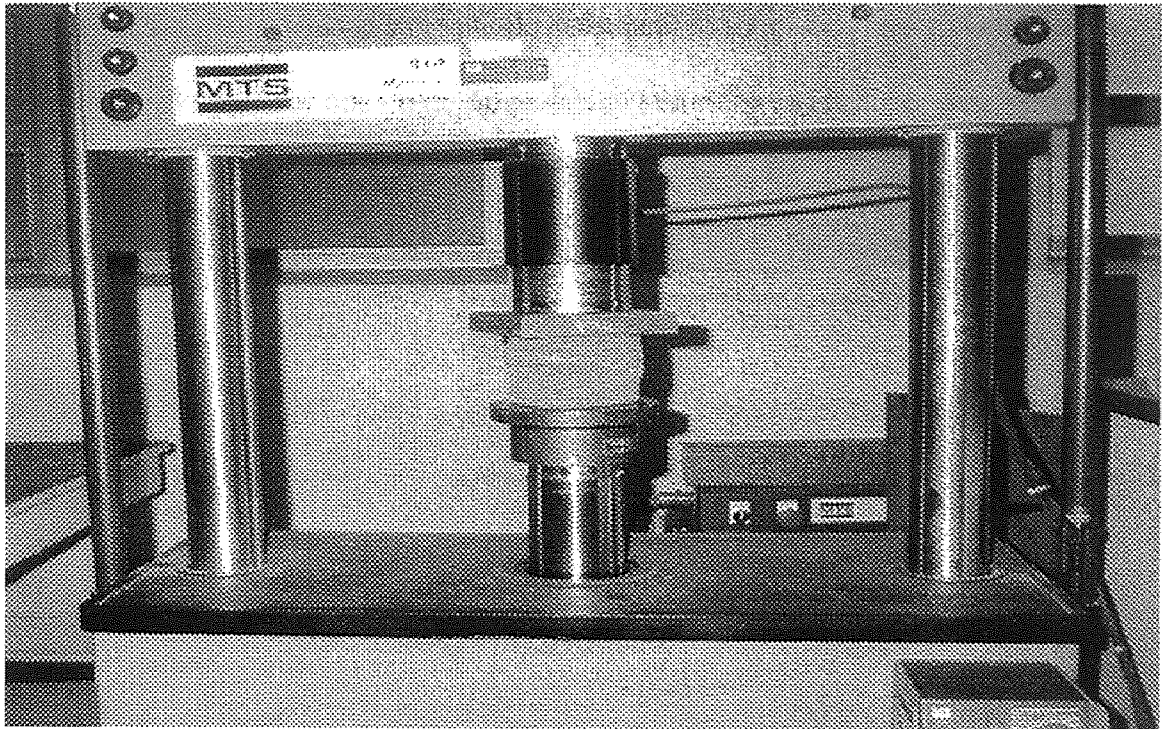
Figure 2.12(a) Manufacturer A Axial Compression
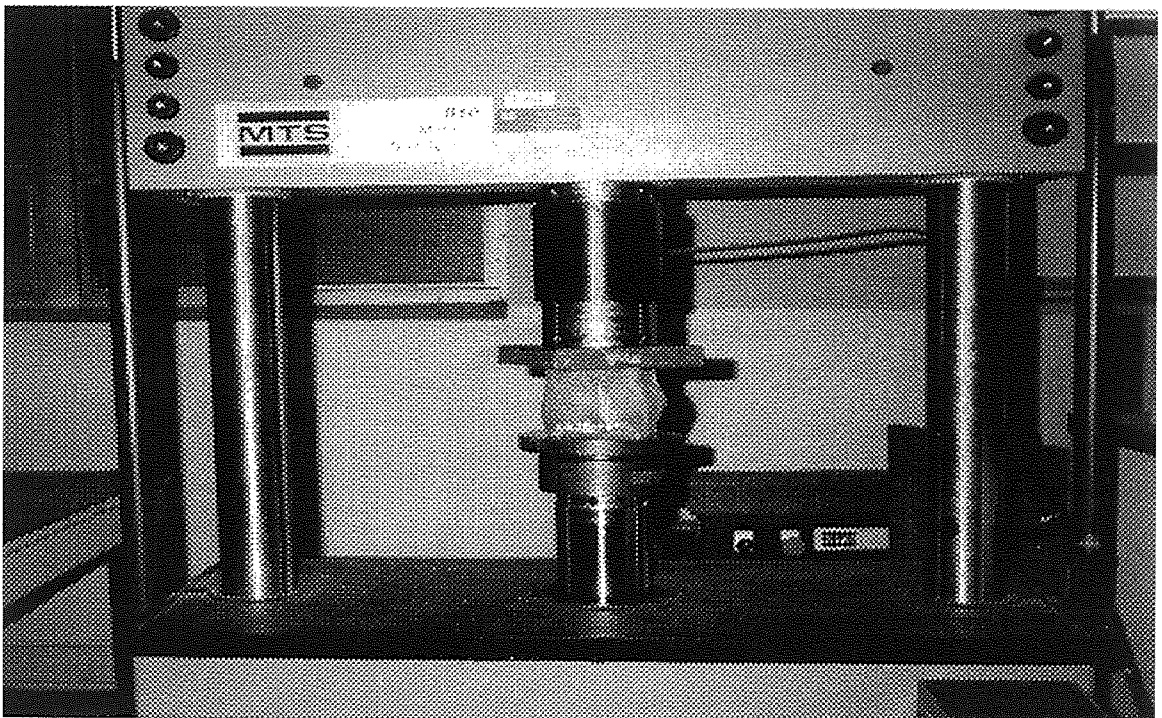
Figure 2.12(b) Manufacturer C Axial Compression

failure, all samples sustained large plastic deformations suggesting that these materials

might be well suited for one - time, large energy absorbing mechanisms such as crash

cushions.

CHAPTER 3

ANALYTICAL VS. EXPERIMENTAL

Two computer programs were developed to predict member behavior by using the proposed material model and the parameters given in Table 2.2. A composite, non-linear section (such as RP) is modeled in axial compression by one program (CRUSH.FOR) and in flexure by the other (BEND.FOR). Numerical integration techniques are used to generate theoretical load-deflection data. The flexural analysis program also generates theoretical moment-curvature and load-rotation data. Both programs assume that there is a distinct division between core and shell and that the section is perfectly rectangular (i.e., roundness of the corners is ignored). The FORTRAN source codes for both programs are included in Appendix A along with the descriptive files that explain their algorithms and implementation.

3.1 Flexure

Appendix B contains Figures B.1 through B.9 which show the bending test results compared with the theoretical curve for all three products. The analytical results agree with the experimental results within 15% for loads less than 80% of the ultimate load for all sections tested. It is suspected that stress concentrations caused by the presence of impurities (mentioned in material tests) effect theory to deviate from test results, particularly at larger loads. The theoretical curve is derived from the coupon tests, but the member is more able to transfer the stress concentrations to adjacent areas than the coupon due to its larger cross-sectional area (i.e., redistribution of stress).

26

The material properties reported by the coupon tests may not be entirely representative of the member behavior. The coupon strain was recorded over a 2" gage length and the net effect of specific, localized stress concentrations occurring in this length cannot be determined because there are several parameters that affect how stress concentrations will change the apparent material behavior. Among these are the ratio of coupon size to impurity size, the ratio of coupon size to member size, the density (frequency) of the impurity distribution and the type of strain gage and gage length. It is not the intent of this paper to investigate these effects but rather to develop and investigate a method for the analysis of composite RP sections.

At larger loads when the material is yielding, the variation between coupon and member behavior will be greater because for greater loads, the coupon can rely less on the impurity bonds. This suggests that for the theoretical member, strength will be affected more than initial stiffness. The fact that the tension strain in the member at failure was greater (typically by 20%) than the maximum coupon strain supports this conclusion. Similarly, the theoretical maximum bending moment (based on maximum coupon tension strain) was less than the maximum moment experienced during testing. To extend the theoretical curves for the purpose of comparison, the program uses the curve fit limit (CFL) as described in Appendix A. The CFL is the maximum coupon tension strain before failure and when the program requires the stress at a strain larger than the CFL, it uses the stress at the CFL. In other words, the curves are extrapolated by assuming pure plastic deformation to take place after the actual observed failure.

Although all of the theoretical curves predict nonlinear behavior, it can be seen that they all anticipate a more linear response than observed in the tests.. It can also be seen

that all but one predict a higher load than observed which may be due to an artificial

strength caused by the plastic CFL assumption noted earlier.

Although it is possible to model the bending of RP sections based on the material

behavior satisfactorily for low loads (Figures B.3, B.7 and B.9), this method seems to

deviate more for higher loads. Because this method is based on simpler, less expensive

coupon tests and does not necessitate separate tests of the entire member for each specific

cross section considered, it is anticipated that it will prove useful for RP analysis.

Additionally, Manufacturer B has reported to now be collecting and sorting the scrap

more carefully so the notion of impurity stress concentrations may soon be irrelevant.

3.2 Compression

Figures 3.1 through 3.3 show the theoretical curves plotted with the axial member

compression test results. The curves can be seen to closely follow the behavior of the

member before buckling of the shell occurs for all three manufacturers. Figures 2.12(a)

and 2.12(b) show two samples at visual failure. Note that Manufacturer A exhibits a local

buckling failure of the shell while Manufacture C seems to have a more general buckling

failure. The test obviously deviates from theory at this point because the possibility of

shell buckling is not considered in the computer program. The agreement between the test

and theory before visual failure occurs indicates that it is possible to predict axial member

behavior with reasonable accuracy in this range but the model gives no prediction of when

the shell buckling might occur.

A simple approximation of the shell buckling load was obtained by considering one

side of the shell to be a simple column supporting a percentage of the total load based on
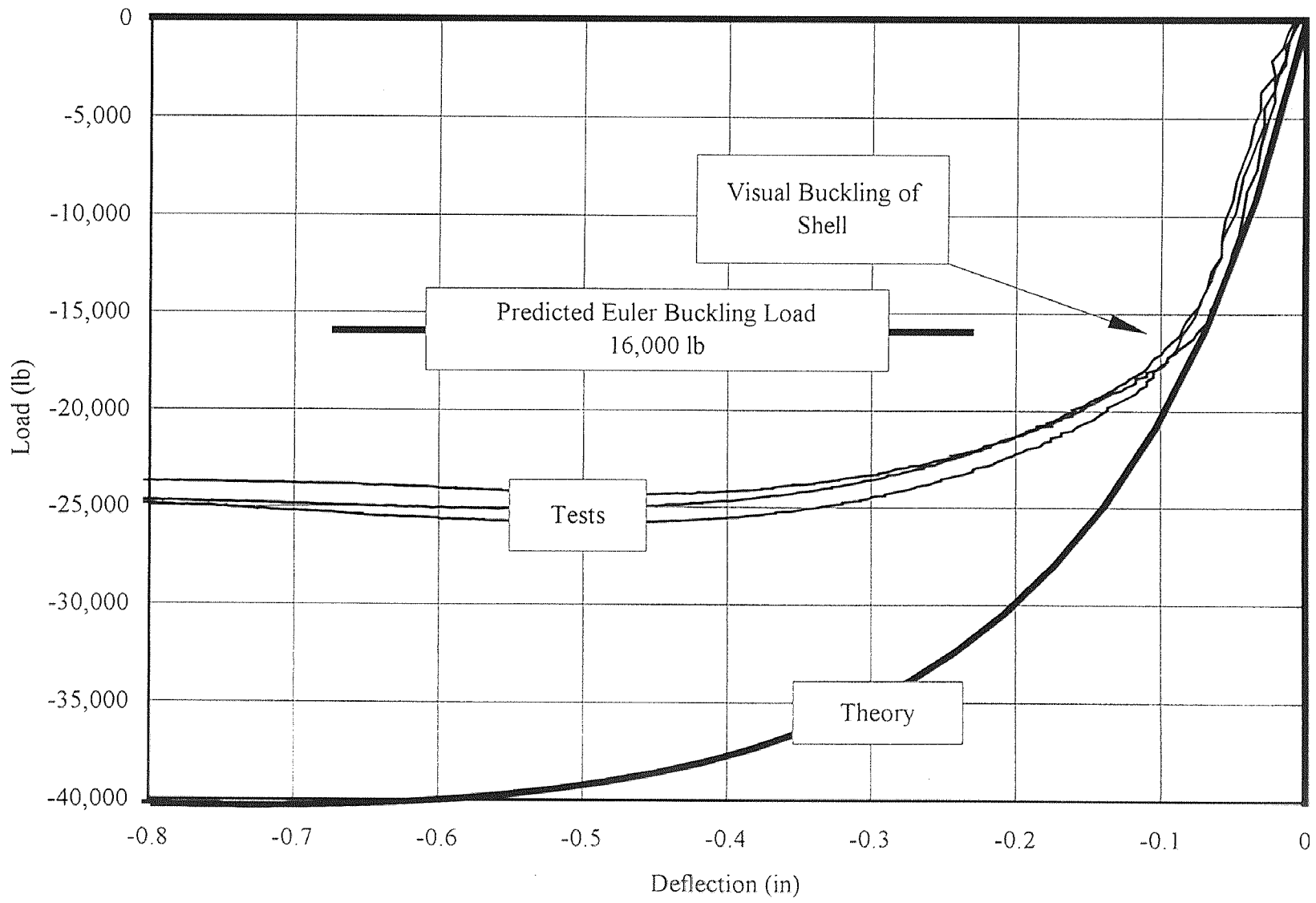
Figure 3.1 Axial Compression of 4x4, Manufacturer A
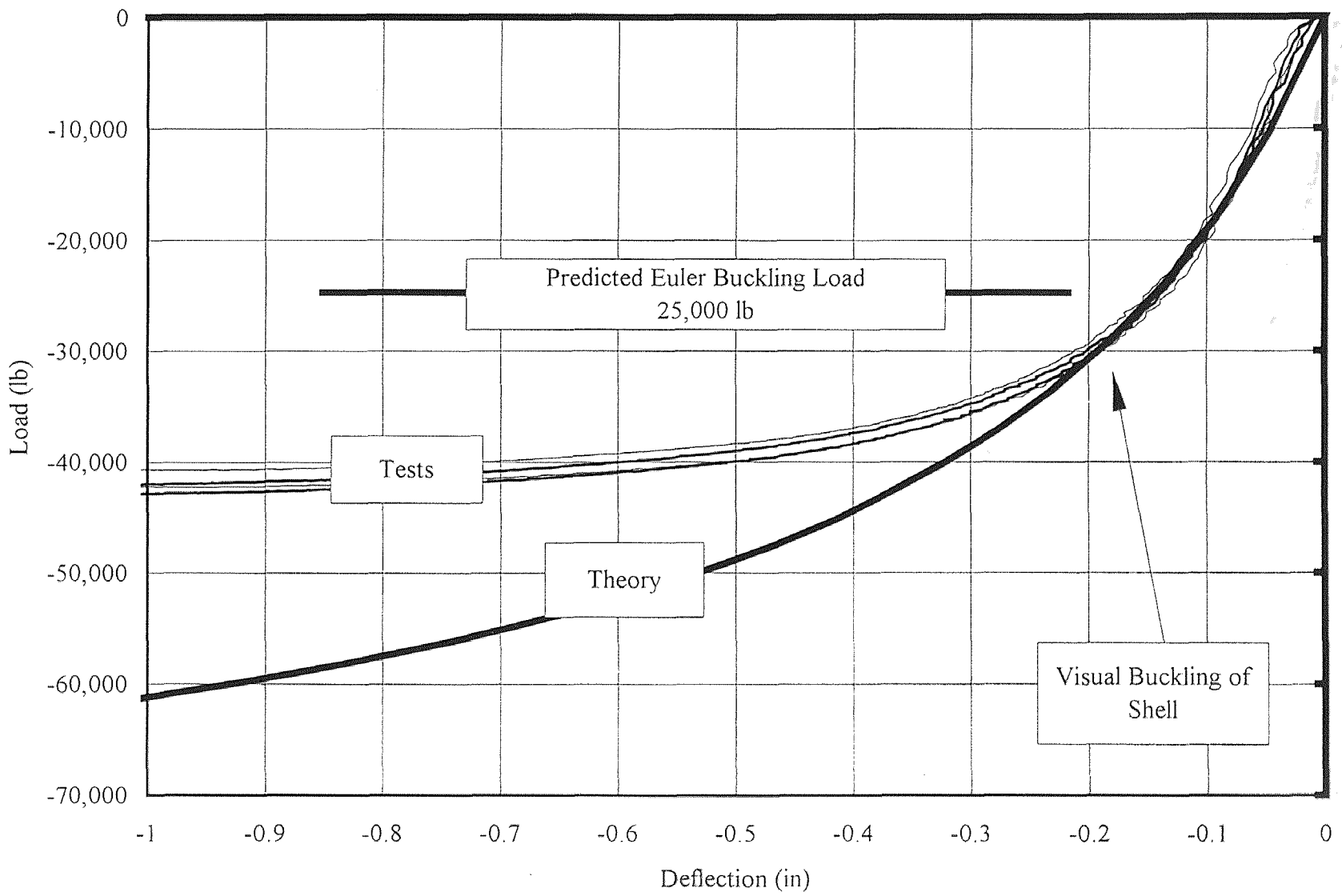
Figure 3.2 Axial Compression of 4x4, Manufacturer B
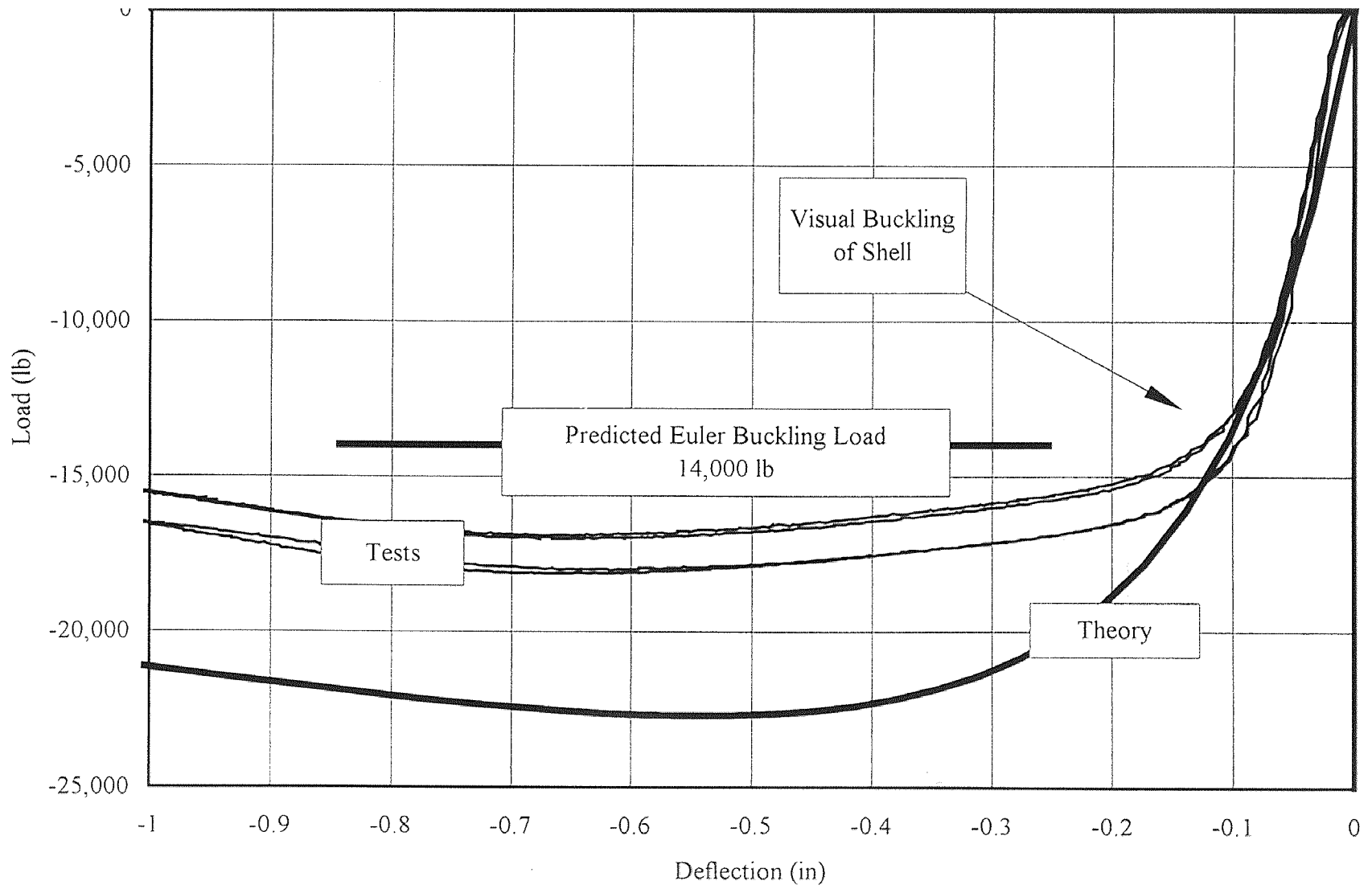
Figure 3.3 Axial Compression of 4x4, Manufacturer C

total cross sectional area and initial E value. The Euler buckling load was computed and the values for each manufacturer are indicated in Figures 3.1 through 3.3 which seems to give a rough indication as to when one might expect this buckling to occur. The values are not as conservative as expected, however, considering the assumptions made which suggests that the mode of failure is more of a localized buckling than a general buckling. It must be emphasized that Euler's approximation as applied here is not only approximate but very subjective and sensitive to one's interpretation of core and shell material. It is presented here only for reference and is not viewed as a good method to predict the ultimate load for RP axial members. A more complex analysis is required if the true behavior is to be considered in detail.

CHAPTER 4

HIGHWAY APPLICATIONS

4.1 Noise Wall

As seen in Table 2.1, the stiffness of RP is generally low; much smaller than concrete or even wood. If current design approaches were to be used, it would be difficult to utilize RP as an economical noise barrier. An advantage of RP, however, is that it can easily be manufactured into various shapes and the cross section does not have to be solid. With this in mind, a new noise barrier design, as shown in Figure 4.1, is proposed. Spacing of the webs was determined through finite element analysis of a typical cell assuming the material to be linear. The proposed design uses shell thickness of 0.5" with an overall depth of 8". A 30 psf (typical AASHTO 80 to 90 mph wind load) applied to a 15' long panel resulted in a maximum deflection of 2.2" and the stresses were below 210 psi. The panel length was increased to 20' causing a maximum deflection of 6.2" and the stresses were still below 360 psi so the linear assumption is still valid. The shell thickness and overall depth of the cross section can also be increased to allow even greater panel length, thus, making more economical designs by further reducing the number of posts.

For typical RP material, the total density (i.e., considering both layers) of the proposed design satisfies the recommendation of 20 kg/m^2 [13] for sound attenuation. It is expected that multi-layering will significantly enhance the sound effectiveness of the wall since layering is the only way to overcome the mass requirement [13]. Prototype panels (Figure 4.2) were assembled from ½" thick RP sheets by fastening them together with screws. They are 8' long and resemble the proposed cross section. The prototype

33
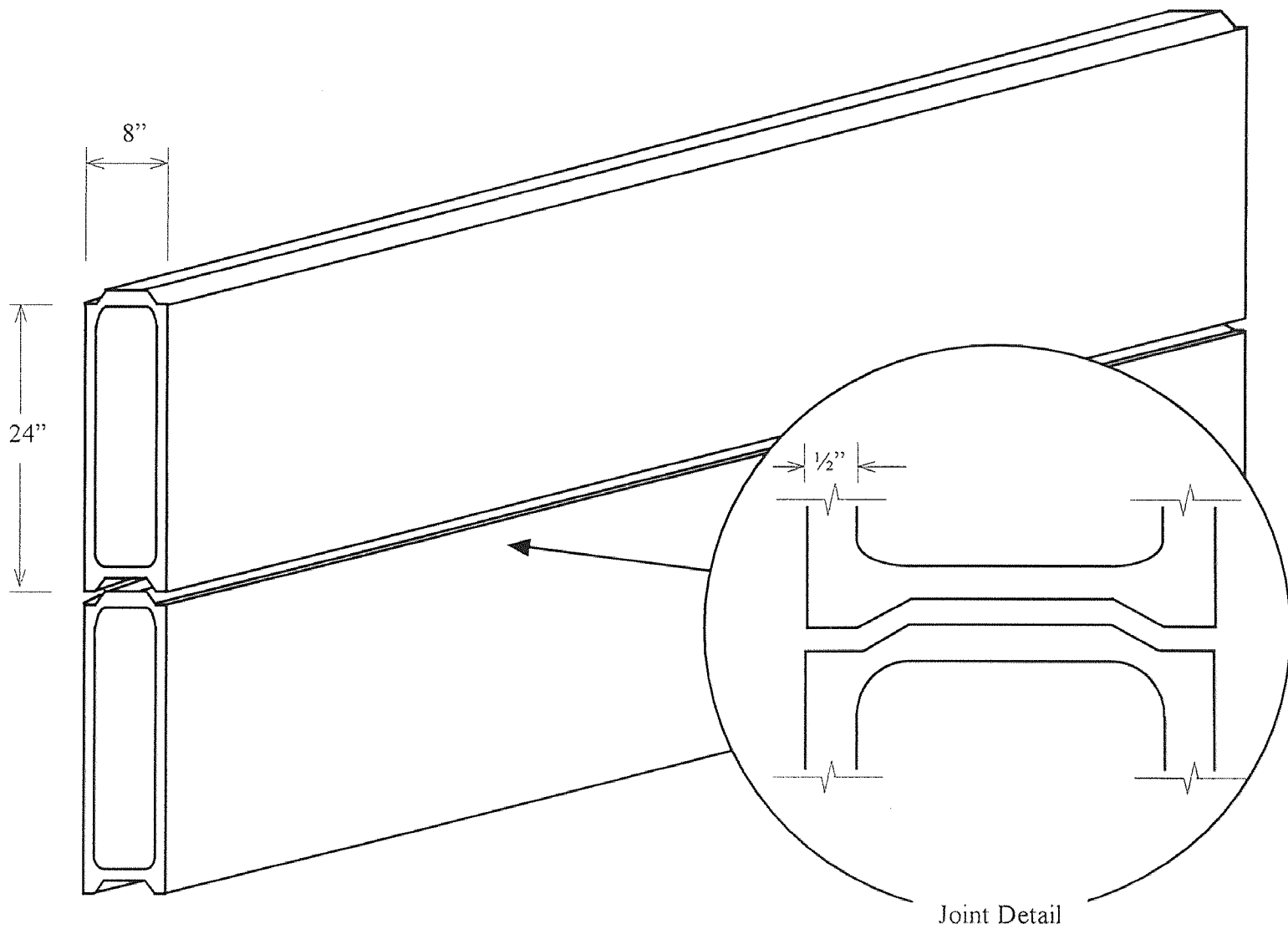
Figure 4.1 Proposed Noise Wall Panels
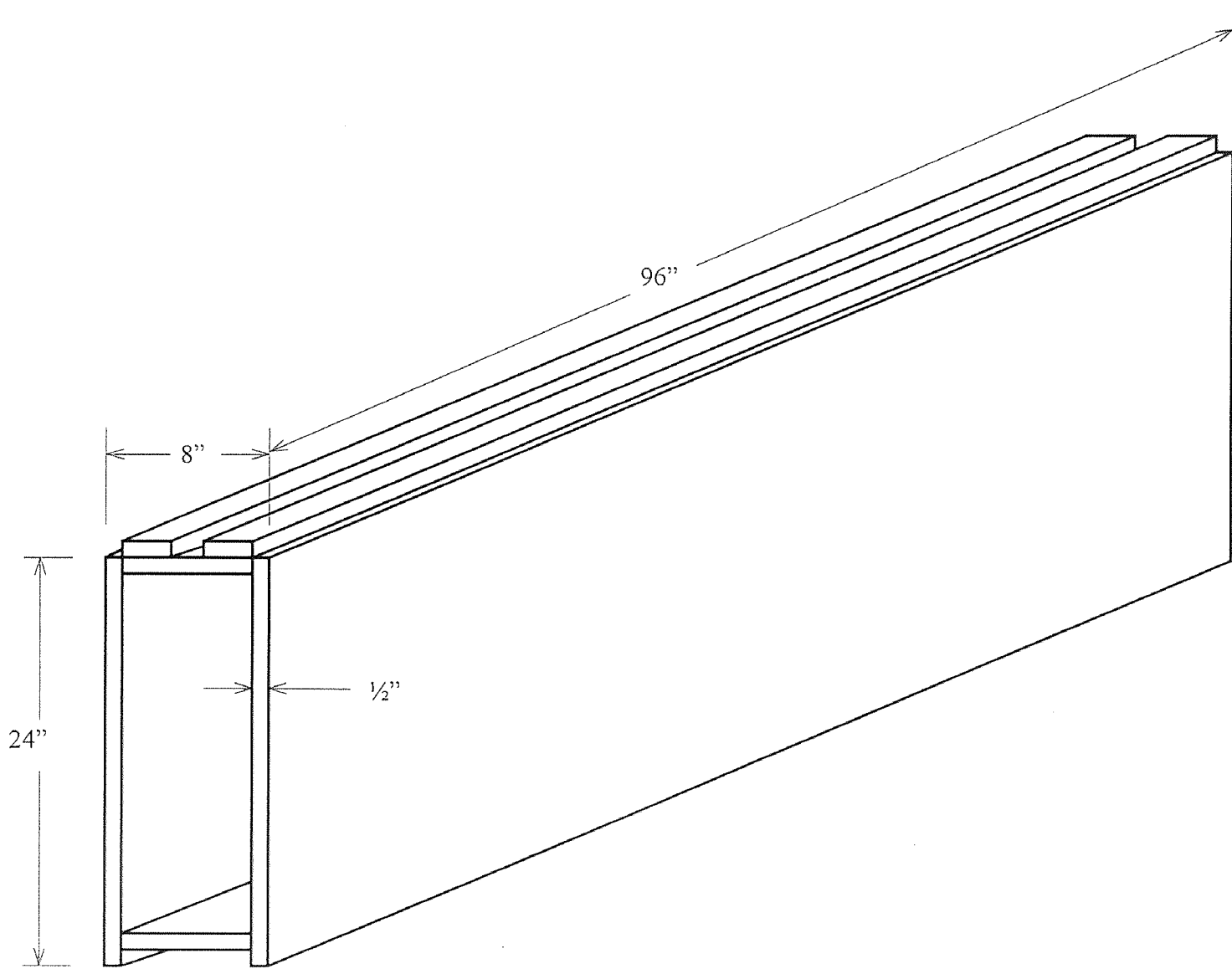
Figure 4.2 Prototype Panel

panels were tested for sound absorption (ASTM C423-90a and E795-83) and transmission loss (ASTM E90-90 and E413-87). The noise reduction coefficient (NRC) is an average of the percent energy absorbed by the test specimen at 250, 500, 1000, and 2000 Hz frequencies. The sound transmission class (STC) of a specimen is a single number that gives an indication of the sound transmitted by fitting the test data to an ASTM defined curve. For the prototype panels, the NRC is 0.10 and the STC rating is 37. Table 4.1 shows these results along with some other commonly used building materials. This shows that these prototype sections are comparable by these standards even though these numbers alone do not give a full understanding of how well a material will perform acoustically in a given situation. The STC and NRC do not reflect, for example, that the prototype panels were noted to perform better at lower frequencies (100 to 250 Hz) of the test range. Large trucks have been noted [14] to generate a majority of their noise in this frequency range.

Table 4.1 Acoustical Properties of Different Materials

Material	NRC	STC
Prototype Panel	0.10	37
6" concrete	0.02	54
1 ¾" wood	0.10	34

Current design guidelines [15] do not specify a minimum STC or NRC for use as a noise wall because it is assumed that the transmission loss of the barrier is large compared to the sound that is diffracted over the barrier. The barrier attenuation is thus considered a function of the site geometry.

4.2 Guardrail Posts

Present technology and design uses road barriers that are made of relatively rigid materials such as steel, concrete or a combination of the two. It is well known, however that flexible but strong designs can absorb more energy, reduce impact deceleration, and minimize the damage sustained by the impacting vehicle and its occupants. Previous research has resulted in designs that incorporate energy absorbing mechanisms (such as the use of rubber energy absorber) and improved the performance of bridge rails [16 - 20]. Due to high initial costs associated with these energy absorbing designs compared to conventional bridge rails, high maintenance costs, and difficulty in attachment to standard bridge decks, these energy-absorbing bridge rails have not gained wide acceptance. The proposed design for road barriers combines the flexibility of plastics (used as posts) with the stiffness of steel rails. Thus, the final product is expected to be functionally superior to current designs.

Analysis of a typical guardrail system was performed using frame models and a linear approximation of 6x8 RP posts. A steel 6x6 box section was used for the rail at a 27" height. With the typical post spacing of 6', it was not possible to satisfy AASHTO's allowable stress requirements. Only when reducing the post spacing to 2' could the 10 kip lateral load be sustained without exceeding the allowable stress of 0.6 times the yield stress ($0.6f_y$). To meet the more demanding AASHTO bridge rail requirements of performance level one (PL-1) or greater, it would likely be cost prohibitive to use RP in a post and rail design. It should be mentioned, however, that PL-1 through PL-4 anticipate relatively rigid barriers [21], and can not be directly used for evaluation of the proposed design which is a flexible one.

In a crash test of a guardrail system, the use of RP posts has been reported as inadequate [22] based on a one-to-one deflection comparison with wood posts. Obviously, RP is much more flexible than wood and if total deflection is compared to wood and this is the only parameter to determine appropriateness of the design, then it will be very difficult or uneconomical to design a guardrail post using RP.

Further investigation of RP for use as guardrail posts should include specific design guidelines to be used for RP. An equivalent replacement of steel posts is not possible because the modulus of elasticity multiplied by the area second moment of inertia (EI) varies by as much as 70 times for the sections discussed. AASHTO suggests an allowable stress design based on a static loading. Using an allowable stress method implies that the rail and posts should sustain no damage under mild events but numerous tests of steel post guardrails [23 - 25] have shown damage to posts in the zone of impact evidencing that the stresses were far beyond allowable. To effectively use RP for posts and capture the high energy absorption potential, the design must be based on recognizing the full strength of the posts in the zone of impact.

CHAPTER 5

FUTURE WORK

To further investigate the appropriateness of the RP for highway appurtenances and advance the general state of knowledge about RP, the following tests and analytical studies should be pursued:

- A more detailed study of the creep behavior which includes longer test duration, different stress levels and different temperatures. It has been seen that creep deflection can be far greater than initial deflection and should be investigated more thoroughly.

- The material model should be verified more exhaustively by comparing the theoretical results with more test results including different materials and cross sections.

- Wind test of full scale panels of the proposed model should be conducted. The wind tests should focus on whether the design loads obtained from current standards are a reasonable predictor of the actual wind loads, and if the flow of wind over the top of the wall causes vortex shedding that might excite the wall and cause it to vibrate.

- Crash worthiness analyses using realistic analytical models by incorporating the proposed material model into an existing program such as BARRIER VII [21].

- Impact tests and verification with analytical procedures.

CHAPTER 6

CONCLUSIONS

Experimental and analytical investigation of RP indicates that it is a viable material that could have structural applications. Material tests revealed that RP is a nonlinear material and the presence of additives such as glass and wood fibers can increase stiffness and reduce ductility. Creep deflection of RP can be very large and freeze / thaw exposure adversely affects materials with wood fibers. It is possible to predict the behavior of RP members with reasonable accuracy for low to moderate load levels based on the material properties. RP is suitable for noise walls but to be efficiently used for guardrail posts, a design methodology based around capturing the large energy absorption capabilities of RP should be considered.

Problems that need to be addressed to ensure the use of RP among structural engineers include quality control, development of standards for testing, design specifications, and long term performance evaluation. Over the last two years, manufacturers have also taken major steps in improving quality and initiating efforts to develop design standards that can be used by structural engineers. Of course, proper dissemination of this work and research as well as developments made at various universities is essential to advancing the state of knowledge.

APPENDIX A

COMPUTER PROGRAMS

The BEND.FOR program for flexure analysis requires an input file to run and generates an output file that contains the input file data, the moment-curvature (M-phi) relation and load-deflection (P-delta) data. The following gives the input file format, details of the program, and the assumptions made in the analysis that the user should be familiar with. The explanation is given in terms of the program variables. The input file must have the following format:

```
h    w    tf    tw    et_stop
A(1)  B(1)  C(1)   D(1)
A(2)  B(2)  C(2)   D(2)
A(3)  B(3)  C(3)   D(3)
A(4)  B(4)  C(4)   D(4)
CFL(1)
CFL(2)
CFL(3)
CFL(4)
method   L   P_lim
```

The above input variables refer to a composite rectangular section with these parameters

h	height of the section
w	width of the section
tf	shell thickness; the flange
tw	shell thickness; the web
et_stop	maximum tension strain produced in bending

The next 16 items are the constants that define the material behavior and fit the equation:

stress = A * e / (B * e^2 + C * e + D), where e = strain. There are four constants (A, B, C, and D) for each type of material behavior. The subscripts for the constants correspond as follows.

1 indicates shell in compression
2 indicates core in compression
3 indicates shell in tension
4 indicates core in tension

The sign convention is positive for tension stress/strain and negative for compression.

CFL (curve fit limit) is the strain that the material property (stress/strain) curve extends to

(negative for compression). The integer number 'method' is the method of loading for the

beam. Possible choices are:

1   Cantilever with concentrated load at the free end
2   Simply supported with a uniformly distributed load
3   Simply supported, one concentrated load at midspan
4   Simply supported, two equal concentrated loads at 1/3 and 2/3 span length

The remaining input items are

L   total length of the beam
P_lim   largest load applied, i.e. the limit of load-deflection data desired.

To describe the analysis algorithm, program variables are listed in single quotes. After

reading the input, 'et_stop' is divided into 'MoPhiSize' equal divisions yielding each 'et',

(tension strain at the outer fiber). For each 'et', a trial & error method is used to size 'y'

(location of neutral axis; from bottom of section) until 'sum_force' (the net axial force; i.e.

Tension + Compression) is less than 'Tol'. If this balance is not found in less than

'time_out' attempts, the program sets 'Flag' equal to the imbalance ('sum_force') and

proceeds to the next 'et'. If the strain in any part of the section exceeds the 'CFL' for that

type, pure plastic deformation is caused in that type by using the stress that corresponds to

'CFL' for all strains greater than this. When the 'CFL' is exceed, 'Plast' is set to reflect this

and written to the 'MoPhi' array as described in OUTPUT FILE.

When 'et_stop' is reached, the program then goes on to compute the deflection of the beam at the point of loading (midspan for method 2). The program uses the internal control constant 'LoDefSize' to divide 'P_lim' into equal divisions. For each load increment 'P', the moment-area method is used to find the deflection by referring to the 'MoPhi' array and interpolating linearly to find the 'phi' corresponding to a given moment. The deflection and rotation at the free end are found by integrating the M/EI diagram (phi) with an interval 'dx'. If the moment corresponding to a particular load exceeds the maximum moment found in the M-Phi array, the message " !! Section will not support this moment ..." is written to the screen and the remainder of the 'LoDef' array is filled with zeros.

The output file contains the 'LoDef' array, the 'MoPhi' array, the input file information, and the internal parameters of the program. The 'LoDef' array contains:

theta   rotation at the end of the beam
delta   deflection at the load point (center for method 2)
P   load corresponding to above theta and delta

The 'MoPhi' array contains

phi   the curvature associated with this moment (et / y)
M   moment generated ('sum_moment')
et   tension strain at outer fiber
ec   compression strain at outer fiber
y   location of neutral axis from bottom
Flag   force imbalance if 'sum_force' is greater than 'Tol' after 'time_out' attempts
      zero if 'sum_force' is less than 'Tol'
Plast indicator of plastic deformation;
      Plast = 0.0000 if CFL has not been exceeded. A one (1) is found in 'type' number of places following the decimal if the CFL has been exceeded in that type.
          e.g. Plast = 0.1000 if CFL has been exceeded in type 1
          Plast = 0.0101 for types 2 and 4

The input file information consists of

geometry	(h, w, tf, tw, et_stop)
constants	(A, B, C, D, for types 1 thru 4)
CFL	(for types 1 thru 4)
loading conditions	(method, L, P_lim)

The internal control constants are

time_out	max number of attempts to find 'y' such that 'sum_force' < 'Tol'
MoPhiSize	size of the MoPhi array
LoDefSize	size of the LoDef array
Tol	allowable tolerance of 'sum_force'
N	number of divisions for each segment of the cross-section
dx	interval used for integration in moment area method

When the program is run, if the file names are not given after the command line, the program will prompt the user for them. The input file is associated with unit 45 and the output file is linked to unit 46.

To change the internal control constants, the user must edit the source code and then compile the program. Any change of the array size should be accompanied by the same change in the declarations section.

The thickness of the area of each element used in the integration varies as y does because the number of elements (N) is constant. The true thickness of the area used is the distance from the neutral axis to the outer fiber divided by 'N'. The user should recognize the significance of exceeding the CFL. Any compatible system of units can be used provided they are consistent throughout.

```
* BEND.FOR: Program to compute deflection in plastic beam
* Declarations
    DOUBLE PRECISION Cnst(4,4), MoPhi(25,7), LoDef(20,3), CFL(2,4)
    DOUBLE PRECISION h, w, tf, tw, y, tA, et, et_stop, ep_outer
    DOUBLE PRECISION force, sum_force, sum_moment, old_sum, area
    DOUBLE PRECISION Tol, Time, Step, Flag, P_lim, P, M, epsilon
    DOUBLE PRECISION x, dx, L, Lp, phi, thetaA, delPA, L_stop, Plast
```

```
      INTEGER count, go, i, k, method, MoPhiSize, LoDefSize,
     + time_out, type

* Program Control Constants
      MoPhiSize = 25
      LoDefSize = 20
      time_out = 50
      Tol = 1D-1
      dx = 1D-1
      N = 100

* Open file and read
      READ (45,*) h, w, tf, tw, et_stop
      READ (45,*) ((Cnst(type,i),i=1,4),type=1,4)
      READ (45,*) (CFL(1,type),type=1,4)
      READ (45,*) method, L, P_lim

* Initializations
      y = h / 3.0
      DO 10 i = 1, 3
   10 LoDef (1,i)=0D0
      DO 20 i = 1, 6
   20 MoPhi(1,i)=0D0

* Begin M - phi
      WRITE (*,*) " Working on Moment - Curvature ..."
      DO 50 k = 2, MoPhiSize
      et = et_stop * DFLOAT(k-1) / DFLOAT(MoPhiSize - 1)
      sum_moment = 0D0
      sum_force = 100D0
      old_sum = 1D0
      time = 1D0
      Plast = 0D0
      Flag = 0D0
      count = 1
      DO 55 type=1,4
   55 CFL(2,type)=0

      DO 51 WHILE ((DABS(sum_force).GT.Tol).AND.(Flag.EQ.0.0))
* Check if sign has changed and adjust y accordingly
      IF (sum_force/old_sum.LT.0) time=time+1.0
      IF (sum_force.LT.0) THEN
       Step = 0.1**time
      ELSE
       Step = -0.1**time
```

```fortran
      END IF
      old_sum = sum_force
      sum_moment = 0D0
      sum_force = 0D0
      y=y+Step

      DO 52 type=1,4
* Shell - Comp
         IF (type.EQ.1) THEN
           tA = (h-y)/N
           ep_Outer = -et*(h-y)/y
           area=tA*tw*2.0
* Core - Comp
         ELSE IF (type.EQ.2) THEN
           tA = (h-y-tf)/N
           ep_Outer = -et*(h-y-tf)/y
           area=tA*(w-2.0*tw)
* Shell - Tens
         ELSE IF (type.EQ.3) THEN
           tA=y/N
           ep_Outer = et
           area=tA*tw*2.0
* Core - Tens
         ELSE IF (type.EQ.4) THEN
           tA = (y-tf)/N
           ep_Outer = et*(y-tf)/y
           area=tA*(w-2.0*tw)
         END IF

      DO 52 i=1,N
      epsilon = DFLOAT(i) / DFLOAT(N) * ep_Outer

      IF ((type.EQ.1).OR.(type.EQ.3)) THEN
       IF ((tA*i).GT.(tA*N-tf)) area=tA*w
      END IF

* Create plastic deformation if > Curve Fit Limits (CFL)
      IF (DABS(epsilon).GT.DABS(CFL(1,type))) THEN
      epsilon = CFL(1,type)
      IF (CFL(2,type).EQ.0) THEN
          WRITE(*,403) " Outside CFL; type",type," at et =",et
          CFL(2,type)=1.
          Plast = Plast + 10**(-FLOAT(type))
      END IF
      END IF
```

```fortran
      force = area*Cnst(type,1)*epsilon/(Cnst(type,2)*epsilon*epsilon
     ++Cnst(type,3) * epsilon + Cnst(type,4))

      sum_force  = sum_force  + force
      sum_moment = sum_moment + DABS(force)*i*tA
52 CONTINUE

      count = count + 1
      IF ((count.GT.time_out).AND.(sum_force.GT.Tol)) Flag=sum_force
51 CONTINUE

* Store results in array
      IF (Flag.NE.0) WRITE (*,*) " sum_force = ",sum_force
     + ," at et = ",et
      MoPhi(k,1)=et/y
      MoPhi(k,2)=sum_moment
      MoPhi(k,3)=et
      MoPhi(k,4)=et/y*(h-y)
      MoPhi(k,5)=y
      MoPhi(k,6)=Flag
      MoPhi(k,7)=Plast

50 CONTINUE

      WRITE (*,401) " ... done!"

* Moment-Area method to compute deflection

      WRITE (*,405) " Working on Load - Deflection ..."
* Method of loading
      IF (method.EQ.1) THEN
      Lp = L
      L_stop=L
      ELSE IF (method.EQ.2) THEN
      Lp = L/2
      L_stop=L/2
      ELSE IF (method.EQ.3) THEN
      Lp = L/2
      L_stop=L/2
      ELSE IF (method.EQ.4) THEN
      Lp=L/3
      L_stop=L/2
      END IF
```

```
* Begin load increments
    go = 1
    DO 40 k=2,LoDefSize
    P=DFLOAT(k-1)/DFLOAT(LoDefSize - 1)*P_lim
    thetaA = 0D0
    delPA  = 0D0
    x=dx


* Begin computations for this load
    DO 41 WHILE ((x.LE.L_stop).AND.(go.EQ.1))


* Find Moment at this location
    IF (method.EQ.1) THEN
     M = P * (L_stop - x)
    ELSE IF (method.EQ.2) THEN
     M = P*x*(L - x) / 2
    ELSE IF (method.EQ.3) THEN
     M = P * L / 4 * (x / L_stop)
    ELSE IF (method.EQ.4) THEN
        IF (x.LE.Lp) M = P * L / 6 * (x / Lp)
        IF (x.GT.Lp) M = P * L / 6
    END IF


* Scan array to find low M
    found=0
    DO 42 i=1, MoPhiSize
    IF ( (found.EQ.0).AND.(MoPhi(i,2).GE.M) ) THEN
    phi = MoPhi(i-1,1) + (M-MoPhi(i-1, 2)) * (MoPhi(i,1)-MoPhi(i-1,
    +1)) / (MoPhi(i,2)-MoPhi(i-1, 2))
    found=1
    END IF
  42 CONTINUE


    IF (found.EQ.0) THEN
    WRITE (*,*) "    !! Section will not support this moment..."
    go = 0
    DO 43 i = k, LoDefSize
    DO 43 j = 1, 3
  43 LoDef (i,j) = 0
    END IF


    thetaA=thetaA+phi*dx
    IF (x.LT.Lp) delPA=delPA+(Lp-x)*phi*dx
    x=x+dx
  41 CONTINUE
```

```
      IF (go.EQ.1) THEN
      LoDef (k,1) = thetaA
      LoDef (k,2) = thetaA*Lp-delPA
      LoDef (k,3) = P
      END IF


  40 CONTINUE

      WRITE (*,401) " ... done!"


********************* OUTPUT TO FILE *********************
      WRITE (46,600) " **** Load - Deflection ****"
      WRITE (46,607) " theta"," delta"," P "
      WRITE (46,707) (LoDef(i,1),LoDef(i,2),
     + LoDef(i,3),i=1, LoDefSize)
      WRITE (46,600) " **** Moment - Curvature ****"
      WRITE (46,617) " phi"," M"," et"," ec"," y"," Flag","Plast"
      DO 60 i=1,MoPhiSize
  60  WRITE (46,717) MoPhi(i,1), MoPhi(i,2) ,MoPhi(i,3), MoPhi(i,4),
     +  MoPhi(i,5), MoPhi(i,6), MoPhi(i,7)
      WRITE (46,600) " *** Geometry ***"
      WRITE (46,627) " h"," w"," tf"," tw"," et_stop"
      WRITE (46,727) h, w, tf, tw, et_stop
      WRITE (46,600) " *** Constants ***"
      WRITE (46,728)  ((Cnst(type,i), i=1,4), type=1, 4)
      WRITE (46,600) " *** Curve Fit Limits ***"
      WRITE (46,729)  (CFL(1,type),type=1,4)
      WRITE (46,600) " ******* Loading ********** "
      WRITE (46,637) " method"," L"," P_lim"
      WRITE (46,737) method, L, P_lim
      WRITE (46,600) " ******* Internal parameters *******"
      WRITE (46,647) " time_out"," M_Phi_Size"," P_Delta_Size" ,
     + " Tol"," N"," dx"
      WRITE (46,747) time_out, MoPhiSize, LoDefSize,
     + Tol, N, dx
      WRITE (*,401) " ... done!"


*************** FORMAT STATEMENTS *************
 400 FORMAT (A,f6.4)
 401 FORMAT (40x,A)
 403 FORMAT (8x,A,14,A,f6.3)
 405 FORMAT (//A)
 600 FORMAT (/,A)
 607 FORMAT (1x,A,3x,A,3x,A)
```

```
617 FORMAT (3x,A,6x,A,7x,A,4x,A,5x,A,3x,A,2x,A)
627 FORMAT (2x,A,3x,A,3x,A,3x,A,3x,A)
637 FORMAT (3x,A,6x,A,7x,A)
647 FORMAT (1x,A,1x,A,1x,A,3x,A,4x,A,3x,A)
707 FORMAT (1X,f6.4,4X,f4.2,2x,f7.1)
717 FORMAT (1X,f7.5,1x,f9.1,2x,2(1X,f7.5),1X,f5.3,1X,f4.1,1x,f6.4)
727 FORMAT (2(1X,f5.2),2(1x,f4.2),3X,f5.3)
728 FORMAT ((e10.4))
729 FORMAT ((f8.4))
737 FORMAT (6X,I1,8x,f5.1,5X,f6.0)
747 FORMAT (2(6X,I3),12x,I2,7x,f4.1,1X,I6,1X,f4.2)

999 STOP
    END
```

The CRUSH.FOR program for axial compression analysis uses the same constants as the

flexure analysis program but only those corresponding to compression. The program uses

the geometry of the section to calculate the force corresponding to a specific strain. The

output file consists of the input information and the theoretical load-deformation data.

The input file must contain the following 12 items.

```
h    w    %core    ec_max
A(1)  B(1)  C(1)   D(1)
A(2)  B(2)  C(2)   D(2)
```

The above variables are defined as follows.

h	height of the cross section
w	width of the cross section
%core	percentage of the total cross section comprised of core material
ec_max	max compression strain expected

The four constants (A, B, C, and D) represent the material behavior in the equation:

$$\text{stress} = A * e / (B * e\char`\^2 + C * e + D)$$

where e represents strain and the subscripts correspond such that

1	indicates shell in compression
2	indicates core in compression

```
* CRUSH.FOR; Program to compute deflection in axial member
*************** Declarations ********************
      DOUBLE PRECISION cnst(2,4), area(3), P_delta(2,40)
      DOUBLE PRECISION h,w,percent_core
      DOUBLE PRECISION ec,ep_inc,ec_max
      DOUBLE PRECISION area, force, sum_force
      INTEGER P_delta_size, type, i

*************** Program constants ***************
      P_delta_size=40

**************** Open files and read *****************
      OPEN (5, file='in.dat')
      OPEN (7, file='out.dat')

      READ (5,*) h, w, percent_core, ec_max
      DO 70 type=1,2
      DO 60 i=1,4
      READ (5,*) cnst(type,i)
  60 CONTINUE
  70 CONTINUE

**************** Initializations *****************


      P_delta(1,1) = 0
      P_delta(2,1) = 0
      ep_inc = ec_max / DFLOAT(P_delta_size - 1)

**************** Begin P - delta *****************

* 1 for shell, 2 for core, 3 for whole section
      area(3) = h*w
      area(2) = area(3) * percent_core / 100
      area(1) = area(3) - area(2)

      WRITE (*,*) " Working on P - delta ..."
      DO 50 i=2,P_delta_size
      ec = -DFLOAT(i-1)*ep_inc

      sum_force = 0
      DO 30 type=1,2

      force = area(type)*cnst(type,1)*ec/(cnst(type,2)*ec*ec
     ++cnst(type,3) * ec + cnst(type,4))
```

```
      sum_force = sum_force + force
   30 CONTINUE

* Store results in array
      P_delta(1,i) = ec
      P_delta(2,i) = sum_force

   50 CONTINUE
      WRITE (*,527) " ... done!"

********************* OUTPUT TO FILE *********************
      WRITE (*,537) " Now writing to fort.",out_file_num," ..."
      WRITE (7,517) " File: fort.",out_file_num

      DO 85 i=1,P_delta_size
      WRITE (*,707) P_delta(1,i), P_delta(2,i)
   85 CONTINUE


      WRITE (7,*)
      WRITE (7,*) " *** Geometry ***"
      WRITE (7,627) " h"," w"," % core"," ec_max"
      WRITE (7,727) h, w, percent_core, ec_max
      WRITE (7,*)
      WRITE (7,*) " *** Constants ***"
      DO 79 type=1,2
      DO 69 i=1,4
      WRITE (7,*) cnst(type,i)
   69 CONTINUE
   79 CONTINUE

      WRITE (7,*)
      WRITE (7,*) " ******* Internal parameters *******"
      WRITE (7,647) " P_delta_size"
      WRITE (7,747) P_delta_size

      WRITE (*,527) " ... done!"
      WRITE (*,*)
      WRITE (*,*)

*************** FORMAT STATEMENTS *************
  507 FORMAT (A,f6.4)
  517 FORMAT (A,I4)
  527 FORMAT (40x,A)
```

```
537 FORMAT (A,I4,A)
627 FORMAT (2x,A,3x,A,3x,A,3x,A)
647 FORMAT (1x,A)
707 FORMAT (1X,f6.4,4X,f15.4)
727 FORMAT (2(1X,f5.2),1x,f4.1,3X,f5.3)
747 FORMAT (6X,I3)

    CLOSE (5)
    CLOSE (7)

    STOP
    END
```
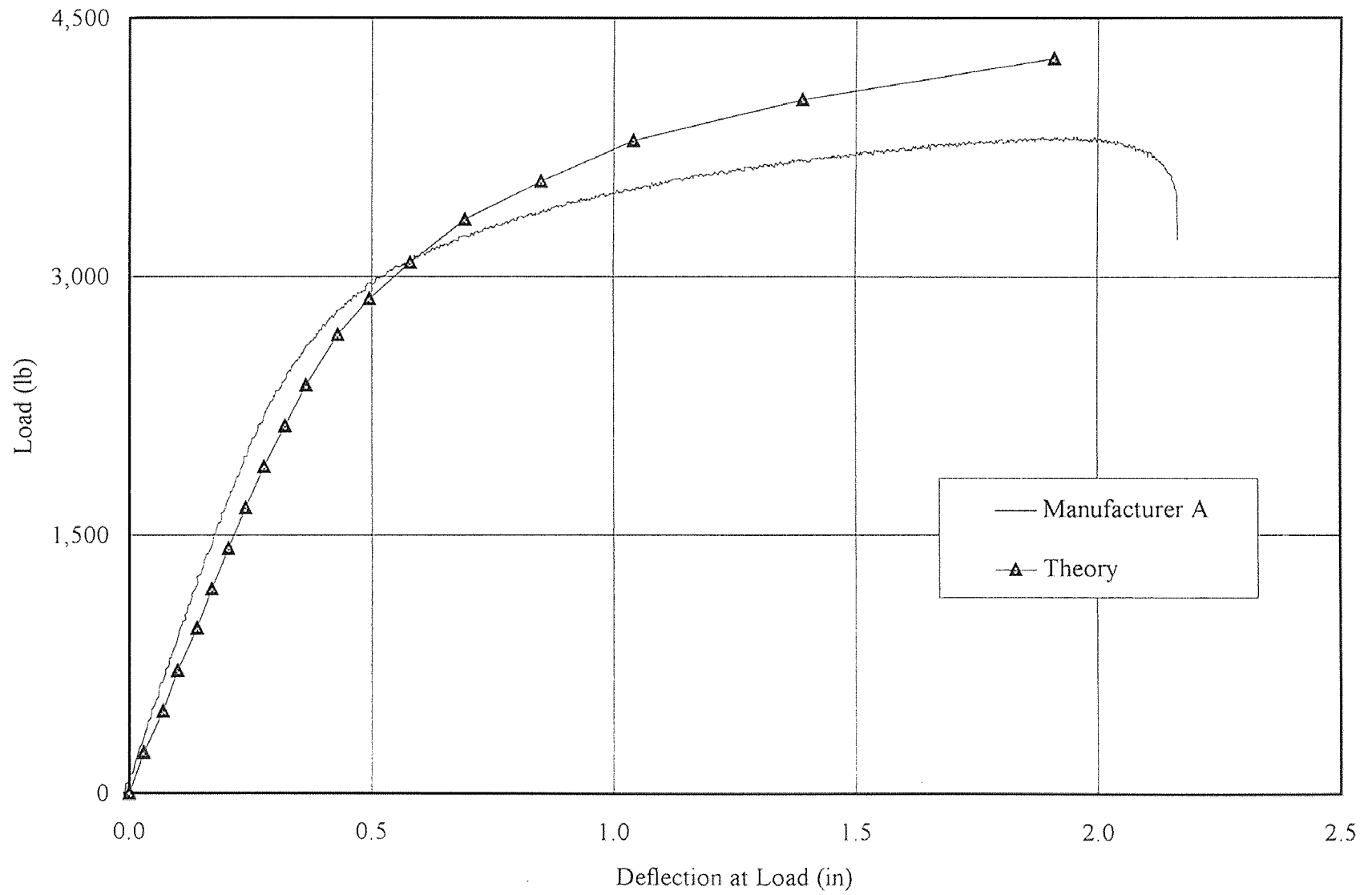
APPENDIX B

BENDING TESTS

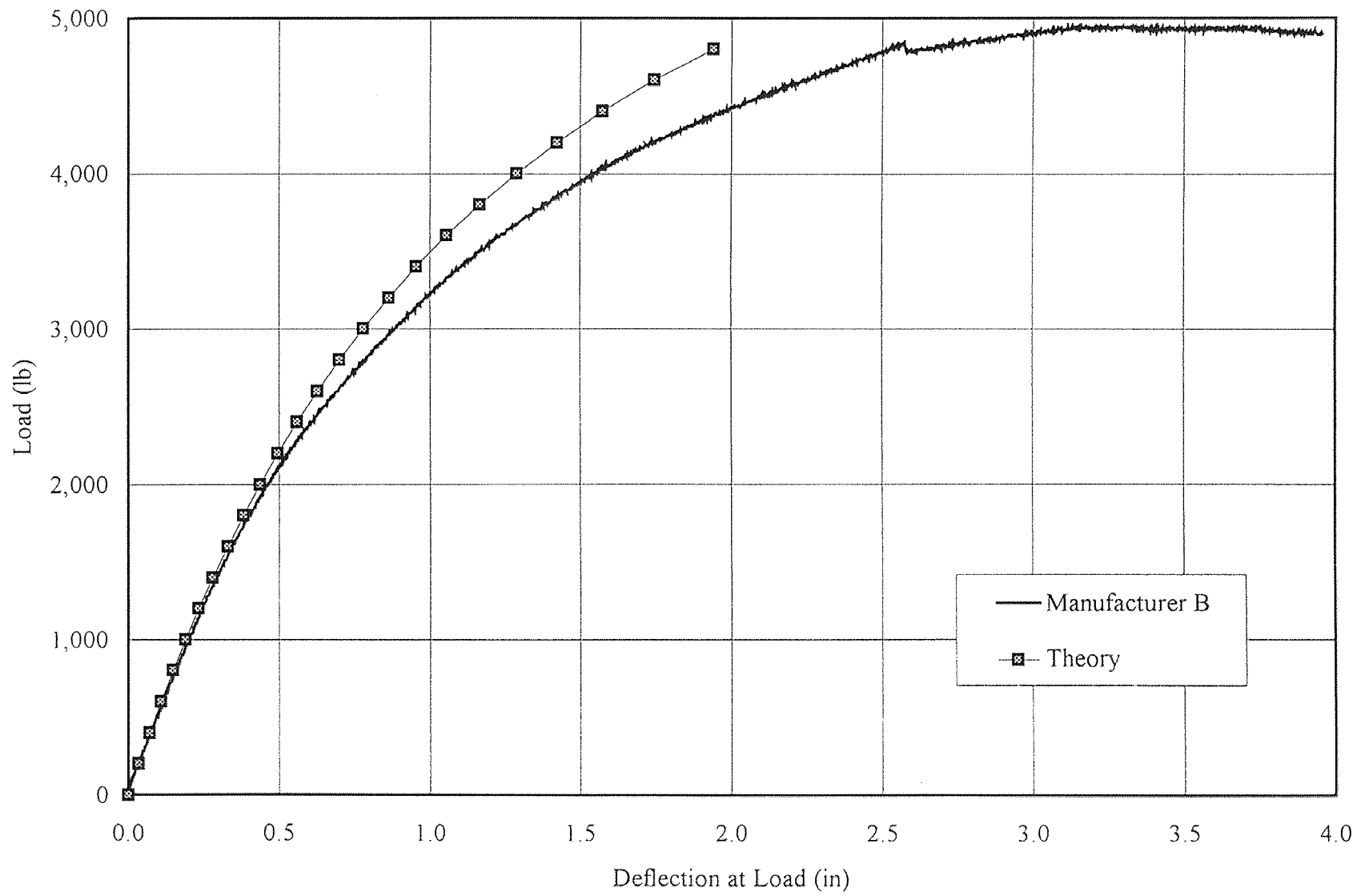**Figure B.1** 4x4 Beam Test Manufacturer A

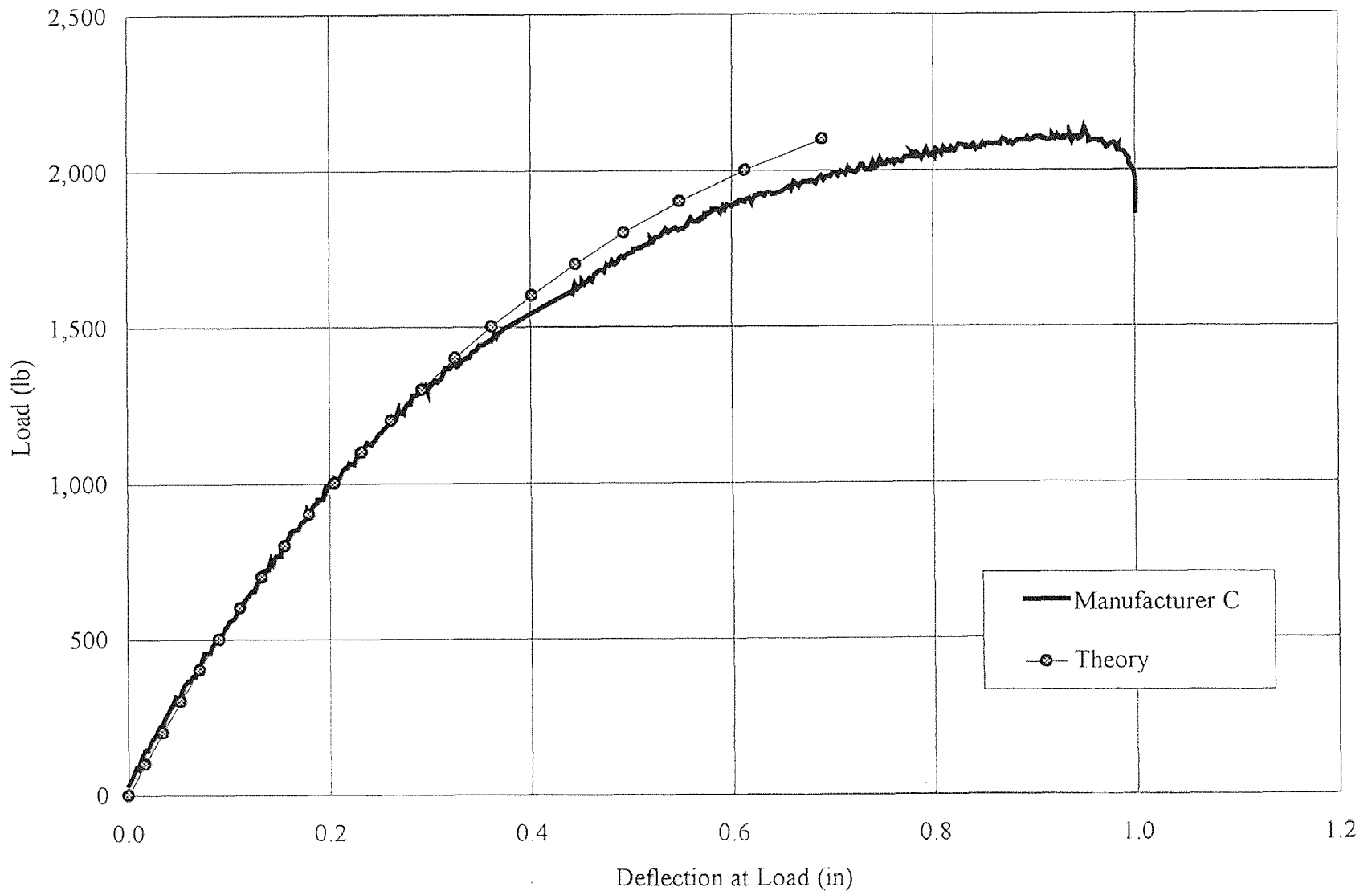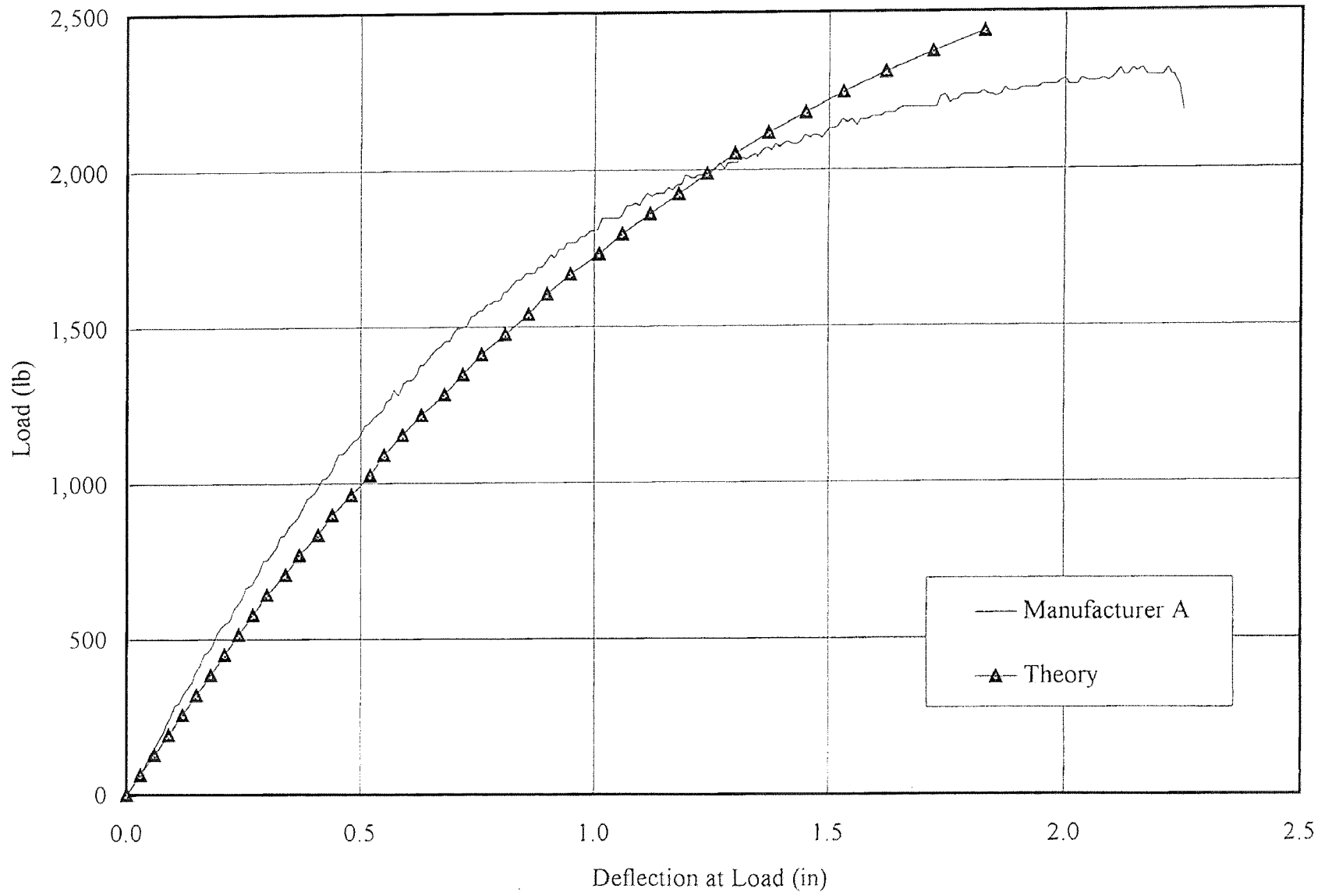**Figure B.2** 4x4 Beam Test Manufacturer B

Figure B.3 4x4 Beam Test Manufacturer C

Figure B.4 6x6 Beam Test Manufacturer A

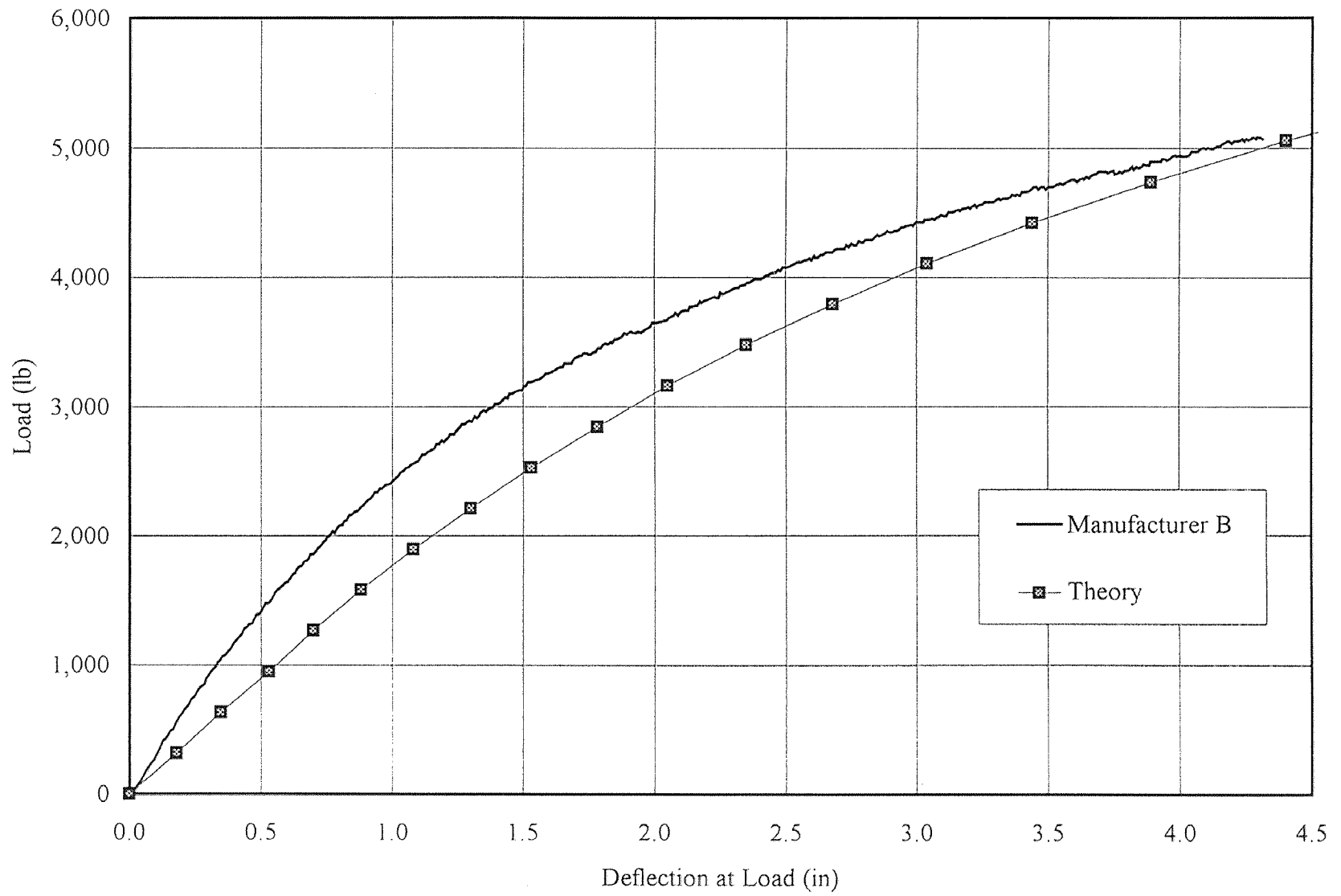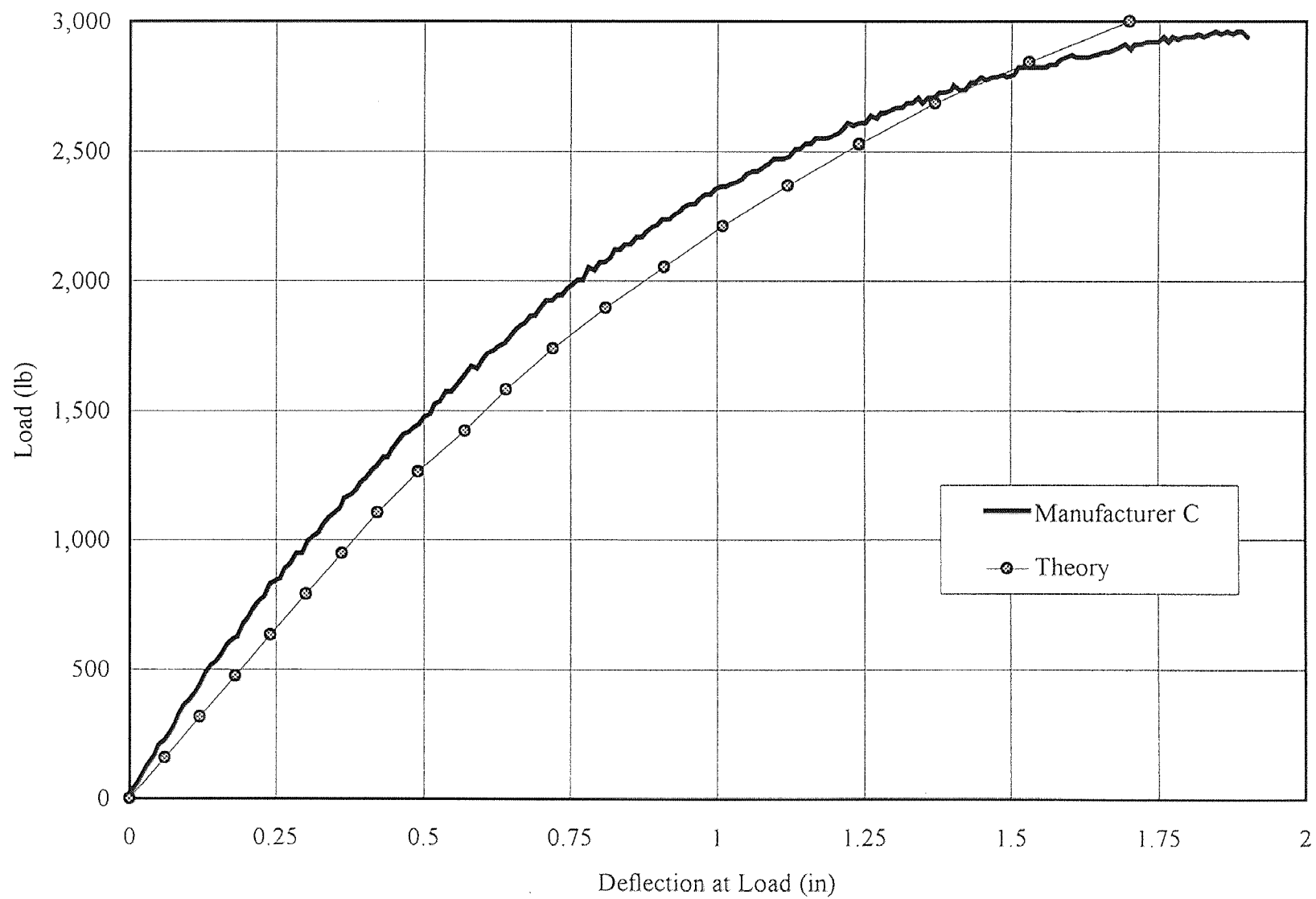**Figure B.5** 6x6 Beam Test Manufacturer B

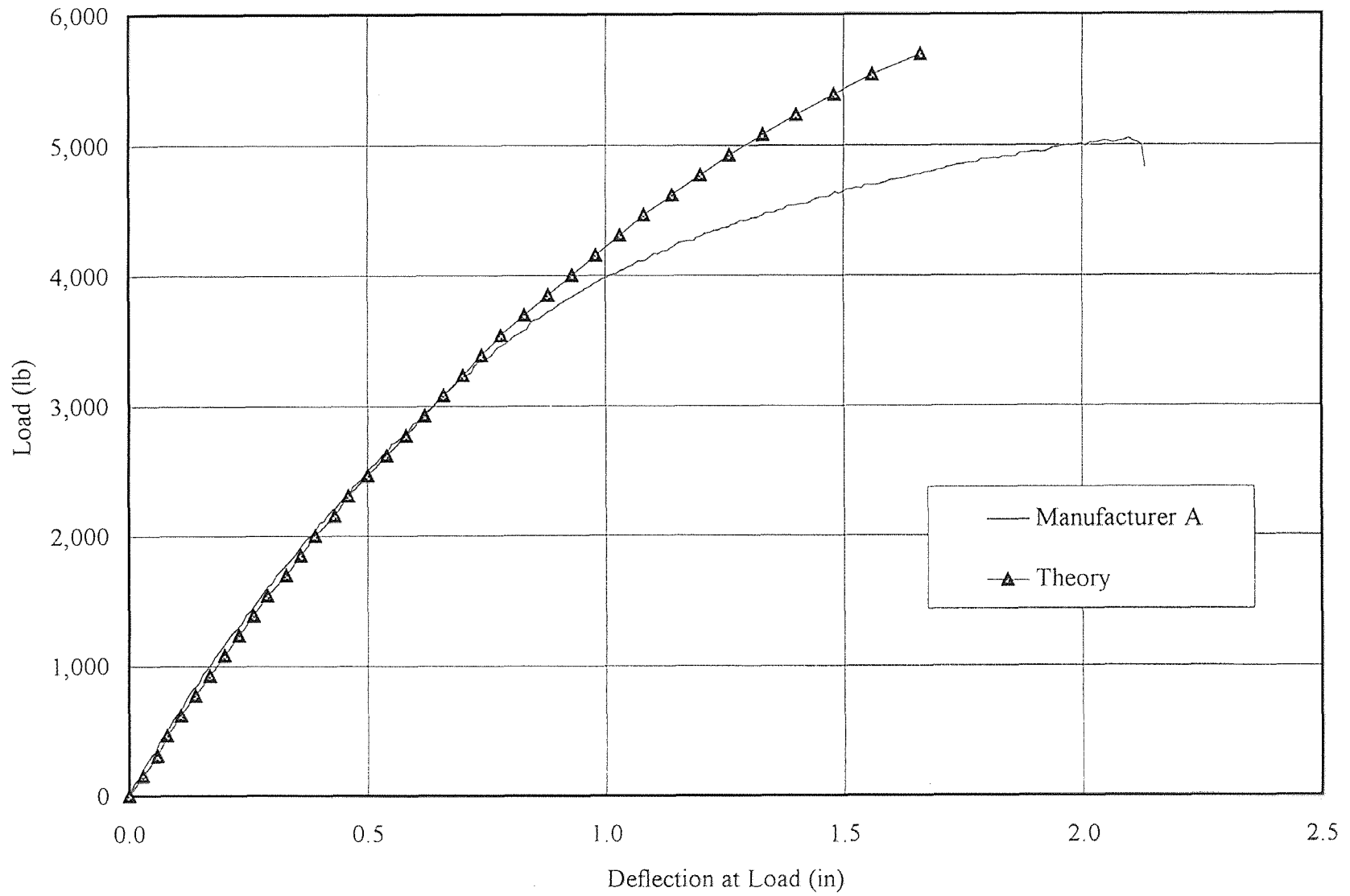**Figure B.6** 6x6 Beam Test Manufacturer C

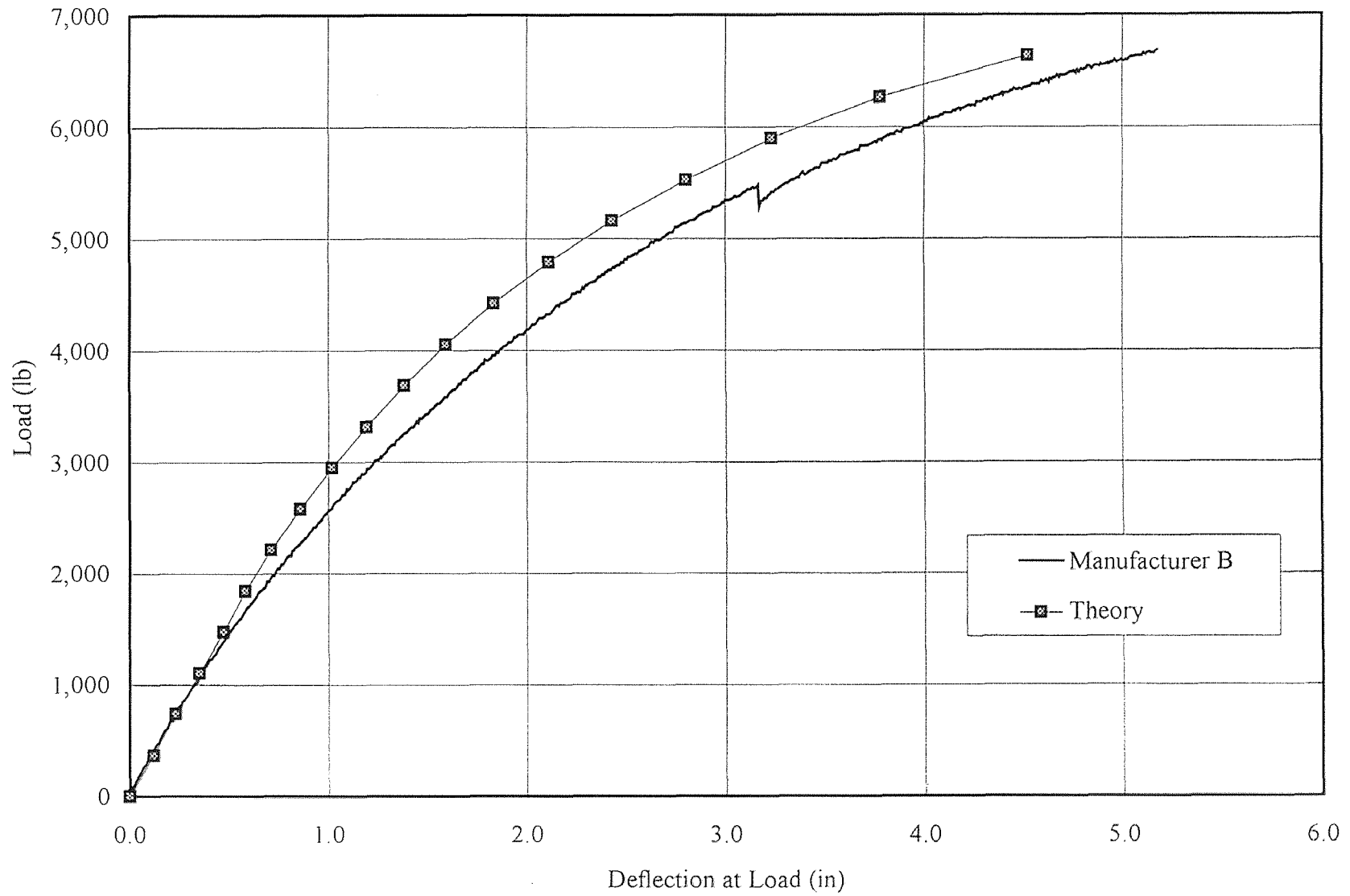**Figure B.7** 6x8 Beam Test Manufacturer A
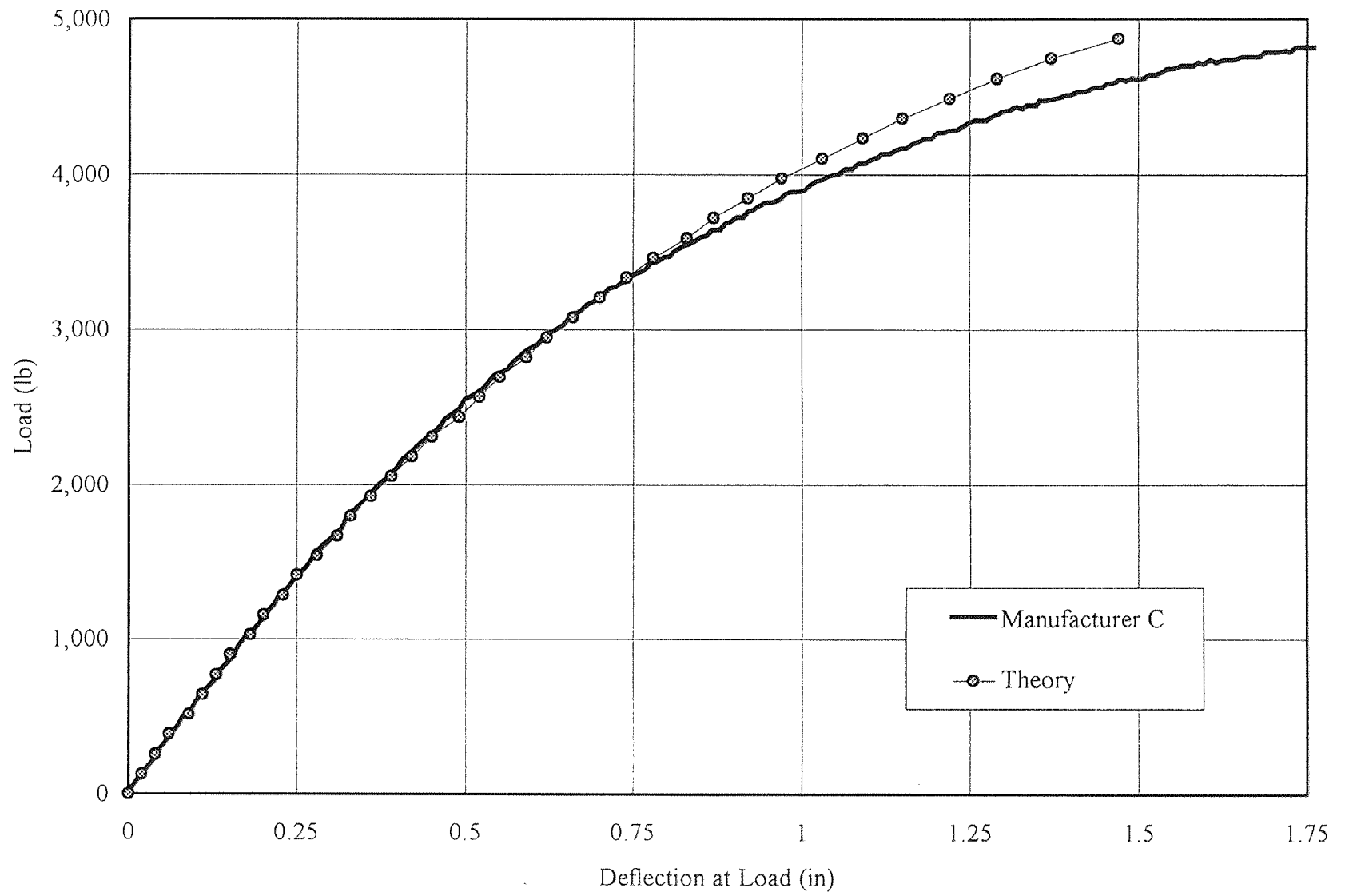
Figure B.8 6x8 Beam Test Manufacturer B

Figure B.9 6x8 Beam Test Manufacturer C

REFERENCES

1. "Furthering The Possibilities," *Plastics World*, April, 1990.

2. "Solid Waste Concerns Spur Plastic Recycling Efforts," *Chemical & Engr. News*, Jan., 1989.

3. Maczko, J., "An Alternative to Landfills for Mixed Plastic Waste," *Plastics Engineering*, April, 1990.

4. "Recycling Mixed Plastics: New Markets," *The Council for Solid Waste Solutions*, The Plastic Recycling Foundation, Washington, D.C., 1992.

5. Bennett, R. A., "Market Research on Plastics Recycling," Technical Report No. 31, *The Center for Plastic Recycling Research*, Rutgers-The State Univ. of New Jersey, 1989.

6. Applebaum, M. D. et. al., "The Properties and Morphology of Fiber Reinforced Refined Post-Consumer Plastics Compounded on a Non-intermeshing Twin Screw Extruder," *The Society of Plastics Engineering*, The 1991 ANTEC Conf., Montreal, 1991.

7. Pearson, W., "Plastics Recycling: The Business," *Plastics Recycling Foundation*, PA, July, 1989.

8. Coomarasamy, A. and Boyd, S. J., "Development of Specifications for Plastic Lumber for use in Highway Applications - Part II," May 1995.

9. Butler, S., Cao, L., and Beatty, C. L., "Engineering Properties of Recycled Plastic Lumber Materials," *Polymer Material Science Engineering*, 1992.

10. McDevitt, C. F. and Dutta, P. K., "New Materials for Roadside Safety Hardware," 1992.

11. Nosker, T. J., Weiss, J. S., Weiss, P., and Greenberg, A., "Toxicity of Construction Materials in the Marine Environment: A Comparison of Chromated-Copper-Arsenate-Treated Wood and Recycled Plastic," *Arch. Environ. Contam. Toxicol.*, 1992.

12. *Numerical Recipes*, Press, W.H. et. al., Cambridge, 1988.

13. Beranek, L. L., *Noise and Vibration Control Engineering*, John Wiley & Sons Inc., New York, 1992.

REFERENCES
(Continued)

14. "Fundamentals and Abatement of Highway Traffic Noise," *U. S. Department of Transportation, FHWA, National Highway Institute*, Report No. FHWA-HHI-HEV-73-7976-1, June, 1973.

15. "Noise Barrier Design Handbook," *FHWA* Report No. FHWA-RD-76-58.

16. Hirsch, T. J., and C. E. Buth, "Testing and Evaluation of Bridge Rail Concept," Final Report, Project RF 3053, *Texas Transportation Institute*, Texas A&M University System, College Station, May, 1975.

17. Kimball C. E., et. al., "Development of a Collapsing Ring Bridge Rail System," Report RD-76-39, *FHWA*, U.S. Department of Transportation, Jan., 1976.

18. Stoughton, R.L., "Vehicle Impact Testing of a See Through, Collapsing Ring, Structural Steel Tube, Bridge Barrier Railing," *Office of Transportation Laboratory*, California Department of Transportation, Sacramento, June, 1983.

19. Beason, W. L., T. J. Hirsch, and J. C. Cain, "A Low-Maintenance, Energy-Absorbing Bridge Rail," *Transportation Research Record* No. 1065, 1986.

20. "Roadside Design Guide," *AASHTO*, Washington, D.C., 1989.

21. Powell, G. H., "BARRIER VII: A Computer Program For Evaluation of Automobile Barrier Systems," *FHWA* Report No. FHWA-RD-73-51, April, 1973.

22. Strybos J. W. P.E. "Recycled Plastics for Roadside Safety Devices", 1995.

23. Faller, R., Ritter, M., Holloway, J., Pfeifer, B., and Rosson, B., "Performance Level 1 Bridge Railings for Timber Decks," *Transportation Research Record* No. 1419, Oct., 1993.

24. Alberson, D., Menges, W., and Buth, E., "Performance Level 1 Bridge Railings," *Transportation Research Record* No. 1500, Jul., 1995.

25. Ross, H., Menges, W., and Bullard, D., "NCHRP Report 350 Compliance Tests of the ET-2000," *Transportation Research Record* No. 1528, Sep., 1996.